

Copyright

by

Arban Uka

2009

**The Dissertation Committee for Arban Uka Certifies that this is the approved version
of the following dissertation:**

**Quantum State Resolved Studies of Copper-H₂ System and
Electronic Spectroscopy of Cu(100)**

Committee:

Greg O. Sitz, Supervisor

Charles Mullins

Manfred Fink

John Keto

Alex Demkov

**Quantum State Resolved Studies of Copper-H₂ System and
Electronic Spectroscopy of Cu(100)**

by

Arban Uka, B.S.

Dissertation

Presented to the Faculty of the Graduate School of

The University of Texas at Austin

in Partial Fulfillment

of the Requirements

for the Degree of

DOCTOR OF PHILOSOPHY

The University of Texas at Austin

August, 2009

Dedication

To my family.

Acknowledgements

First I would like to thank Prof. Greg O. Sitz for his enormous help during my years in his lab. His enthusiasm is contagious when explains the work in the lab to visitors, undergraduate and graduate students, and to professors. He has a friendly, serious and professional approach to all of his students and puts a lot of effort and time in both teaching and advising them.

I would like to thank the members of my dissertation committee, Professors Charles Mullins, Manfred Fink, John Keto and Alex Demkov for carefully reading this thesis and suggesting changes.

I would like to thank Dr. Leah Shackman for teaching me how to run the main experiment, Dr. Jonghyuk Kim for teaching me the two-laser experiment and the insightful and helpful long time friend Shengyuan Zhang. Many students have worked in the lab on different projects over the years and I would like to thank them for the discussions that we have had, for the help they have provided and for the fun that they added to the lab. They are Rick Hankins, Anne Smith, Robynne Hooper, Elisabeth Siebert, Joel Meyers, Jonathan Ganc, Andrew Hill, Eric Irrgang, Victor Chua, Matthew Wilde. I thank also everyone on the second floor of Physics Department for their help when I have knocked on their doors, especially the Dr. Downer, Dr. Raizen and Dr. Keto labs. I thank Dr. Watson Henderson, who was always ready to answer questions I had about running the lab. I thank the machine shop, the electronics shop and the cryogenics shop for providing parts that we needed in the lab and also for teaching me a great deal. Jack Clifford's work and his help to me and to all students has also been greatly appreciated. Finally, I thank my family for their support, patience and love.

Quantum State Resolved Studies of Copper-H₂ System and Electronic Spectroscopy of Cu(100)

Publication No. _____

Arban Uka, Ph.D.

The University of Texas at Austin, 2009

Supervisor: Greg O. Sitz

Hydrogen quantum state resolved energy losses upon scattering from copper are studied using molecular beam techniques and quantum state-specific detection methods. Also clean copper and hydrogen and oxygen covered copper surfaces were studied using electron spectroscopy.

There are many questions about the nature of molecule-surface dynamics and the processes. The relative role of the different degrees of freedom in the reaction and the importance of non-adiabatic effects have been two of these questions. These two questions motivated this work. Energy loss in the elastic scattering of H₂($v=1, J=1$) and H₂($v=0, J=1$) molecular quantum states is measured as a function of incident translational energy at two surface temperatures. The energy loss process is shown to agree to the Baule classical model for energy ranges 74-150 meV for the excited vibrationally state

and 74-125 for the ground vibrational state. Results suggest that translational energy is more effective than vibrational energy in the observed process. Theoretical models have been able to explain several processes using nonadiabatic models where friction coefficient tensor is included. Results in this thesis suggest that the energy loss in the elastic scattering is a nonadiabatic one.

Electron spectroscopy studies showed that the surface plasmon intensity is very sensitive to surface contamination. Using this property, surface-only sensitive virtual temperature programmed desorption (VTPD) is developed. A better understanding of unique behavior of hydrogen covered Cu(100) was gained.

Table of Contents

List of Tables	x
List of Figures	xi
Chapter 1 Introduction.....	1
1.1 Why surfaces?.....	1
1.2 Metal-hydrogen systems	7
Chapter 2 Experimental Setup	10
2.1 Sample preparation	11
2.2 Main Chamber	12
2.3 Molecular beam preparation.....	13
2.4 Pumping and probing of the molecular beam using optical methods....	15
2.5 Electron spectrometer	22
Chapter 3 Quantum State Resolved of H ₂ Scattering from Cu (100).....	27
3.1 Background work.....	27
3.2 Experimental results.....	30
Chapter 4 EELS and LEED studies of Cu (100).....	41
4.1 Clean Cu(100)	42
4.2 H/Cu (100) and the virtual TPD	52
4.2.1 H/Cu(100) and Copper reconstruction	52
4.2.2 EELS studies and “virtual TPD” of H/Cu(100).....	56
4.3 O/Cu (100).....	67

Chapter 5 Conclusions.....	72
References.....	74
Vita	83

List of Tables

Table 3.1 Translational energy loss for H ₂ (v=1, J=1) and H ₂ (v=0, J=1) upon scattering from Cu(100) surface at 173K.	34
Table 3.2 Translational energy loss for (v=1, J=1) H ₂ and (v=0, J=1) H ₂ upon scattering from Cu(100) surface at 573K.	37
Table 4.1 Hydrogen, deuterium and oxygen molecular flux at P=10 ⁻⁶ Torr and times needed to expose 1ML on Cu(100).....	56

List of Figures

Fig. 1.1 Contour plot showing 2D PES for H ₂ dissociation above the bridge site of Cu(100) calculated by Kroes. The zero of energy corresponds to two H-atoms in the gas phase. This plot is taken from reference 24.....	4
Fig 1.2 Degrees of Freedom for a hydrogen-metal system. “Me” are the metal atoms.	6
Fig. 2.1 General view of the experimental setup in the vacuum chamber	11
Fig. 2.2 i) Typical TOF of the vibrational ground state. ii) Typical TOF of the vibrationally excited state (two laser) iii) Typical TOF measuring the incident and scattered (v=1, J=1) state. Times are with respect to the chopper trigger signal.	19
Fig. 2.3 (i) Measurement of initial and scattered energy for (v=1, J=1). The MB is pumped and then probed by the probe laser which ionizes them. One TOF is ≈ 1μs wide in order to ionize the scattered signal too. (ii) Measurement of the incident energy of (v=0, J=1). MB is pumped from (v=0, J=1) to (v=1, J=1) at the peak time and the pumped pulse is probed by probe laser. Sample is taken out of the MB path. (iii) Measurement of the energy of the scattered (v=0, J=1). (v=0, J=1) is pumped and then is probed by the probe laser. Note that in all cases the probe laser is set at corresponding ionizing wavelength of (v=1, J=1).....	20
Fig. 2.4 The shadow created by the wire is shown (Diam.=0.38mm) The blue small circles represent the probe laser. The drawing is not to scale.....	21
Fig. 2.5 General schematics of LEED apparatus and required electrical connections. [29].....	23
Fig 2.6 EELS measurement of copper sample. Energy of the incident beam is 330 eV. Inset shows surface plasmon (Σ), bulk plasmons (β ₁ , β ₂) and Auger electrons (58 eV).	24
Fig. 2.7 Auger measurement of copper sample before cleaning. Copper features are seen at 58 and at 105 eV. Carbon contamination is seen at 270 eV.	25
Fig. 2.8 Virtual TPD (VTPD) of H/Cu(100). Intensity of the surface plasmon and its derivative is shown. The derivative is proportional to the rate of desorption. T=βxt (Heating rate is constant)	26
Fig. 3.1 Peak times as a function of probe laser position. From this graph we can calculate the velocity of the incident and scattered beam, change in the kinetic energy of the beam and the distance of the sample with respect to the laser.	31
Fig. 3.2 Incident and scattered energy for H ₂ (v=0, J=1) and (v=1, J=1) quantum states of hydrogen upon scattering from Cu(100), T _{Cu} =173K. The lines are fits to the Baule equation in the	

low energy region where the data shows close to linear dependence. For comparison the energy exchanged for H₂ scattering from one copper atom (n=1) and an infinite mass atom (n=∞) are shown. 33

Fig. 3.3 Incident and scattered energy for H₂ (v=1, J=1) and H₂ (v=0, J=1) quantum states of hydrogen upon scattering from Cu(100), $T_{Cu} = 573$ K. Data is fitted to the Baule Eqn. in the low energy range. $n_{(v=1, J=1)}=0.5$, $n_{(v=0, J=1)}=0.7$. For comparison the energy exchanged for H₂ scattering from one copper atom (n=1) and an infinite mass atom (n=∞) are shown..... 35

Fig. 3.4 Incident and scattered energy for H₂ (v=1, J=1) and H₂ (v=0, J=1) quantum states of hydrogen upon scattering from Cu(100), $T_{Cu}=573$ K. Data is fitted to the Baule Eqn using n-values found for the cold sample. 36

Fig. 4.1 A typical electron energy loss spectrum for copper taken for a primary beam energy of 300 eV at T=-100°C. The elastic peak, the surface plasmon at a loss of 6.3 eV and the two bulk plasmons at losses of approximately 18 eV and 28 eV are seen. 43

Fig. 4.2 Sample energy loss spectra taken after every hour. The copper Auger electron peak at 58 eV and the EELS peaks are seen. The intensity decreased continuously with time. Each scan took about 8 minutes to acquire. 45

Fig. 4.3 Consecutive energy loss spectra of surface and bulk Plasmon every 70 minutes with E=330eV and E=0 eV. For the first two the copper Auger peak is shown. 1 vs 2, 2 vs 3, 3 vs 4 and 4 vs 5 are shown with the condition as shown in each graph. 48

Fig. 4.4 EEL spectrum data taken every one hour. --■-- is the first scan. --◆-- is the scan after 8 minutes. --▲-- is the scan after 4 hours. The decrease of surface plasmon intensity in the first 4 hours is approximately 30%..... 50

Fig. 4.5 Surface plasmon intensity as a function of time as it is exposed to the electron beam. The background has been subtracted. The inset shows the early time data on an expanded scale. 51

Fig. 4.6 LEED for clean and reconstructed Cu. i) Clean Cu E=148 eV. ii) Streaky pattern of Cu(100) LEED just before getting reconstructed. $E_e=120$ eV. iii) Reconstructed Cu (100) upon dosing H atoms at -150°C. $E_e=138$ eV. iv) LEED of H/Cu(100) at E=89 eV. Dosed at -100°C. 54

Fig 4.7 (i) Conventional TPD using mass spectrometry. (ii) Virtual TPD obtained by taking the derivative of the intensity of the surface plasmon. 58

Fig. 4.8 Surface plasmon intensity and Virtual TPD are shown for: (i) Surface cleaned followed by the heating-cooling cycle and exposed to electron beam at $z=0.68''$ for 10 minutes ($-\Theta-$), measurements at $z=0.60''$ with no prior electron beam exposure ($-\blacktriangle-$). (ii) Measurements are compared for different cooling times. Relatively rapid cool down ($-\Theta-$) and slower cool down ($-\blacktriangle-$). (iii) Repeated measurements at the same sample spot. First cycle ($-\bullet-$), second cycle ($-\blacktriangle-$). In each case the cooling time was ≈ 20 min. 61

Fig. 4.9 Virtual TPD spectra. (i) Two consecutive TPD after 50 ML H_2 doses. (ii) Two TPD after 50 ML doses with a 250 ML dose in between. (iii) Two consecutive TPD after 50 ML doses..... 63

Fig 4.10 (i) Virtual TPD after 250 ML exposure. (ii) Mass spectrometer signal after 400 ML exposure. Desorbed hydrogen can be seen at $365^\circ C$ 66

Fig 4.11 LEED of O/Cu(100) at different energies after 460 ML exposure and clean surface pattern..... 68

Fig 4.12 (i) Virtual TPD of O/Cu(100) after it is exposed to hydrogen the first time (ii) Virtual TPD of O/Cu(100) after it is exposed for the second time to hydrogen..... 70

Chapter 1 Introduction

1.1 WHY SURFACES?

There is a great need to understand the physics of surfaces and in particular the physics of the interactions of molecules with surfaces. Whenever we prepare anything such as food, or fix something, instead of using many hands we put everything on a table and work with them. We can think the same way about the surfaces of materials which we use every day. These surfaces can be smooth or rough and a definition of the surface which comprises it all would be: “the first molecules that we interact with upon hitting a material.” Using this definition what we are really saying is that whatever you do you have to first “pay your dues to the surface,” you have to knock “at the door.”(We are saying interact and not touch, pretty much all the surfaces are just felt but not all are touched: interaction on a distance.)

For all of the work in this thesis, the surface under consideration is held in an ultra-high vacuum (UHV) chamber and the gas is delivered to the surface in the form of a molecular beam. For a reaction to occur certain molecules have to be at a certain place and a certain time and the presence of a surface on the path of a molecule just provides a place in space where a molecule is going to be thus making it easier to add another molecule for a possible interaction. If a molecule sticks on this surface then the time available to meet another molecule increases thus increasing the probability for interaction. Another aspect of which we can make use is that the symmetry present in the bulk is broken at the surface. The atoms at the top layer have less atoms to make a bond

with thus making the surface chemically active. This covers just the catalytic, if there is one, aspect of the surfaces.

Another aspect of much interest is the dynamics of molecules in the vicinity of a surface. Experimentally, it is difficult to send a molecule to a surface and know exactly the full nature of the interaction. The molecule may be on the way to a locally stepped surface, to a corrugated one or to a disordered one. As is the case in every field, the experiment gives the results for a certain input but offers little information on the intermediate steps. The reason is that the interaction happens in such a small time scale that it is nearly impossible to monitor. For example, the energy might go from translational degree of freedom to the vibrational degree of freedom through an intermediate rotational state excitation. Molecules inherently have many degrees of freedom (DOF) and each of them would affect the experimental outcome in a different way. To identify the relative importance of DOF on the interaction we need to do quantum state resolved measurements [1]. In the work in our lab we monitor the quantum states of the molecules before and after scattering from transition metals. Having only the information about the final quantum states of the molecules does not offer much information about the complete adsorbate-substrate interaction. The molecule can cause some change in the substrate and likewise the substrate can cause some change in the molecule. To understand the full dynamics the only thing that can be done is to try building theoretical models of these interactions. To make the comparison between theory and experiment easier it is helpful to use well ordered surfaces where one expects similar behavior over the entire interaction region. Even for well ordered surfaces McCormak et al. have found different reaction probabilities for different sites (top, hollow, bridge) on the surface but now they are repeatable over the entire surface [2].

They have found that adding vibrational energy to the molecule increases the reaction probability at the top sites and this is explained by the barrier for H₂ dissociation on Cu(100) being late for top site. (A late barrier is one which happens at relatively large interatomic distances. The barrier shown in Fig. 1.1 is a late barrier.) Theorists start with a well-ordered surface and a molecule and then calculate the potential function for the interaction. This process gives the so called Potential Energy Surface (PES) which is a function of all of the degrees of freedom of both molecule and substrate. An example of a PES calculated for H₂/Cu(100) is shown in Fig 1.1. This is a contour plot vs r , z and is called an elbow plot. r is the bond length of the hydrogen molecule and z is the distance of the molecule from the surface. To make meaningful comparison with theory, experimentalists use well structured crystals of metals and of semiconductors. And if we are to improve the first definition of a surface given above we have to say that the surface is the top most few atomic layers of a solid.

After selecting the surface next step would be to choose the molecule. It is good to start with the simplest of all and many research groups have done so: using hydrogen. While hydrogen is the simplest molecule it still brings difficulty for theoreticians because it exhibits very strong quantum effects [3]. Theoreticians have to solve the problem quantum mechanically including as many of the DOF's as they can. To measure the effect of all DOF's on the interaction the experimentalists try to vary them one at a time. Further understanding of specific processes can be and has been gained by comparing results of hydrogen with deuterium [4]. These two molecules have the same electronic potential energy surface but different masses. The D₂ molecule having a larger mass for the same conditions would have smaller kinetic energy and move more slowly into a surface and this would give more time for interaction. For example, dynamical steering is

an effect observed in hydrogen-surface systems where higher kinetic energy molecules have less time to be acted upon by the potential gradient and so instead of being steered to non-activated paths would hit the repulsive part of the potential [5]. Shackman et al. studied HD scattering on both benchmark systems for activated and nonactivated surfaces: copper and palladium [6]. One additional variable is that the surfaces can be

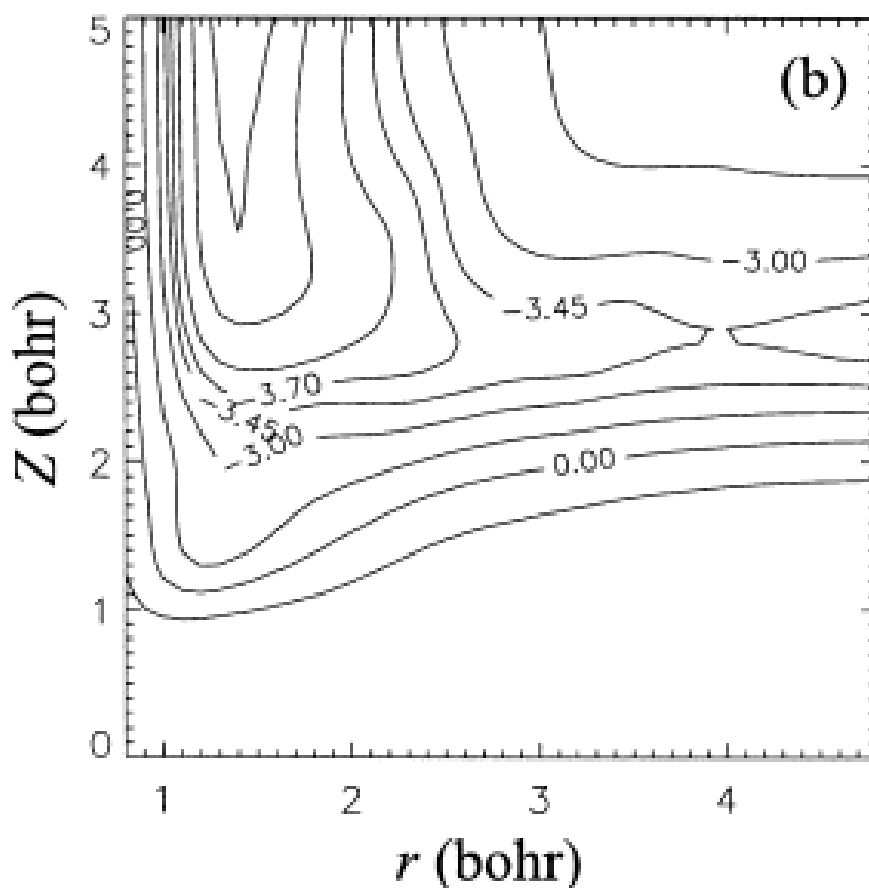


Fig. 1.1 Contour plot showing 2D PES for H₂ dissociation above the bridge site of Cu(100) calculated by Kroes. The zero of energy corresponds to two H-atoms in the gas phase. This plot is taken from reference 24.

modified and the PES changed and so we might see different dynamics and/or reaction probabilities on them. For example, the H_2/Pd (111) system doesn't have a precursor [5] while the H_2/Pd (111)-V does [7]. So modifying the surfaces in a controlled manner can make them more or less likely to react with certain molecules.

Over the years experimental results and theoretical calculations have been continually compared: sometimes agreement is good, other times it is not. As the years passed and experimental methods have improved, higher quality data have been offered to theory as a challenge to reproduce the observations. Also the theory has been predicting the outcome of experiment and offering new ideas to experimentalists. The common goal is to generate a more complete idea of the whole picture of the complex interactions. The most important and difficult aspect of the theory of surface-gas dynamics is the calculation of the PES. The PES for a diatomic molecule and any surface has six degrees of freedom (DOF) as shown in Fig. 1.2: the coordinates x , y , z of the center of mass with respect to the surface atoms, r : the distance between the two atoms which accounts for the vibrational energy of the molecule and two angles θ with respect to the z -axis that corresponding to the rotational energy of the molecule and Φ which describes the orientation of the molecule with respect to the x axis on the surface. Theoretical models are not complete and the role and relative importance of the six different DOF are not fully known. Having to consider many possible reactions or channels where energy is lost makes it clear that what is really needed are well-done experiments to compare with the calculations. Unfortunately many regions of PES are inaccessible to the experiment [2] so saying the final answer only by calculations is difficult for now.

Dynamical Model

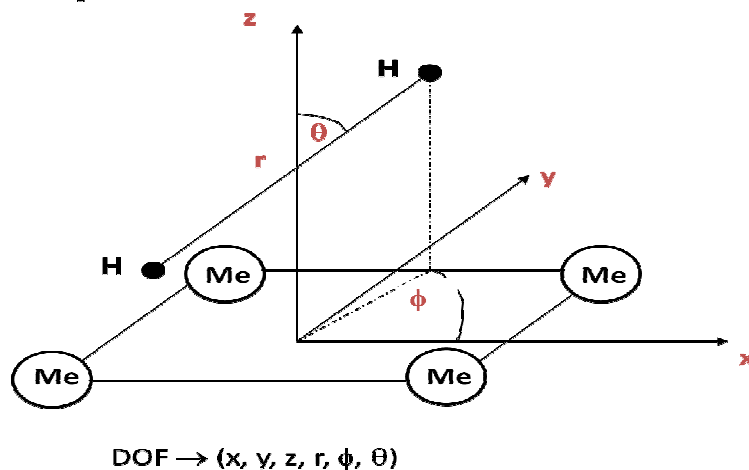


Fig 1.2 Degrees of Freedom for a hydrogen-metal system. “Me” are the metal atoms.

PES calculations have contributed a great deal to our understanding of many important aspects of gas-surface dynamics. There are cases where for two very similar systems the sticking coefficient is up to 2 orders of magnitude different in the thermal energy range. For example, from experiment it is known that N_2 molecules with thermal energy adsorb with a much higher probability on W(100) than on W(110). In the process of finding the reason for the difference between those two systems density functional calculations performed by Alcudin et al. showed that this arises from the characteristics of the PES far from the surface which resulted in a greater chance for the molecule to trap in a precursor well on W(100). [9] Development of experimental methods has helped observe critical aspects of reactions on the surface. In another example, Mitsui *et al*, using STM observed that H_2 requires three or more adjacent vacancies rather than two to adsorb successfully on Pd (111) [10, 11] and so making this process third order rather than a second order. This result was contrary to what has been widely accepted.

1.2 METAL-HYDROGEN SYSTEMS

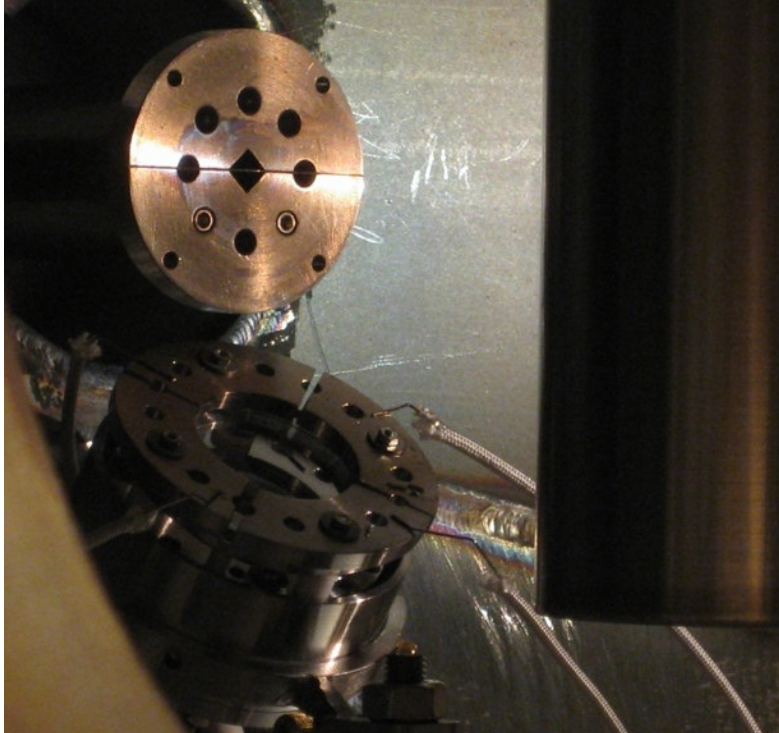
In the studies of molecule-surface systems focus has been on the diatomic molecules and this is explainable because of smaller number of DOF to work with and monitor and of less possible energy transfer channels within the DOF. Among the diatomic molecules hydrogen has been the first choice for many reasons. Among those: it is a simple, light molecule which can be solved quantum mechanically with essentially no approximations [12], it has far-spaced rotational energy states because of its small moment of inertia and this is helpful when studying the rotational degrees of freedom, and it has been established both experimentally and theoretically that the phonons are relatively unimportant [5, 12]. The importance of studying hydrogen is reflected on the vast amount of research in the literature for the past 30 years. Understanding hydrogen-metal systems is fundamental in work on catalytic processes [13, 14], hydrogen storage, processes ranging from the heating of a space vehicle on reentry into the atmosphere, to the precision etching of metallic features during integrated circuit fabrication. After extensive studies the understanding of the processes is not complete. The possible processes that can happen in molecule-surface interaction are: i) reflection of the molecule with no change in the molecule's DOF also called elastic scattering, ii) excitation or relaxation of the molecule upon scattering also called inelastic scattering, iii) dissociative adsorption and iv) diffusion on the surface. The first three processes are important because they involve energy exchange between the degrees of freedom of both substrate and adsorbate and a quantitative description of this exchange has been a long standing question in the surface science field. To answer such a question a great amount of work has been done by theoreticians and it has been proven that classical and quasi-

classical treatment of H₂-metal system often does not provide an accurate description. There have been experiments and theoretical studies that have focused on a certain aspect or a certain DOF and both agreement and disagreement have existed. For example, the steering effect in nonactivated H₂-palladium system was predicted by theory [5] has been observed experimentally [15] thus giving hope that the full picture of the interaction is understood.

Most of the time theoreticians in their calculations have considered the H₂-metal system to be in the electronic ground state. Thus the electronic DOF were not considered in the energy transfer analysis. The early work of Persson and Hellsing [16] and Langreth [17] showed electronic excitation is responsible for the widening of the lifetime of the vibrations of the molecules adsorbed on metal surfaces. The mechanism involves the excitation of an electron-hole pair. More recent experimental work [18-21] showed that the energy of the adsorbate can be transferred very efficiently into the electronic DOF of the substrate. It is ubiquitous that the electronic structure of the substrate would greatly affect the adsorption. Using density functional calculations Hammer et al. compared the sticking of H₂ on Ni, Pt, Cu and Au [22]. They showed that nobleness of the material was related to two factors: the degree of the filling of the antibonding states on adsorption and the degree of the orbital overlap with the adsorbate. They concluded that the sticking probability depends largely on the metal d-states, where the d-band is with respect to the Fermi level. Harris et al. showed that the dissociation of hydrogen at transition metal surfaces at large distances is controlled by the translational energy of the molecule. With enough energy the Pauli repulsion is overcome as the molecule comes to separation smaller than 3 a.u. where dissociation has been proven to be facilitated by the d band electrons of the substrate [23]. When considering the scattering problem and the possible

energy losses and/or energy transfer for the molecule Luntz's work has been more relevant. (Scattering processes would be explained better by his model) In their calculations nonadiabatic effects were included as a friction. They calculate a friction tensor for H₂/Cu(111). The elements of this tensor η_{zz} , η_{dd} and η_{dz} are friction coefficients corresponding to translational energy, vibrational energy (damping) and the coupling of translational and vibrational energy respectively. Calculations done on the vibrational relaxation of hydrogen molecules upon scattering showed that the process was a nonadiabatic one [24, 25]. Our work will try to shed new light on the nature of the processes in a scattering experiment in H₂/Cu system. The scattering experiment results presented in this thesis will test the η_{zz} coefficient.

Chapter 2 Experimental Setup



**Main Chamber entrance aperture with a horizontal wire and the
Channel Electron Multiplier Array (CEMA)**

The apparatus used for the work described in this thesis consists of three main parts. A ultra high vacuum (UHV) surface science chamber, a supersonic molecular beam source and two laser systems: pump and probe laser. Most of the devices used have been designed and developed by Dr Sitz and his students in the past 20 years.

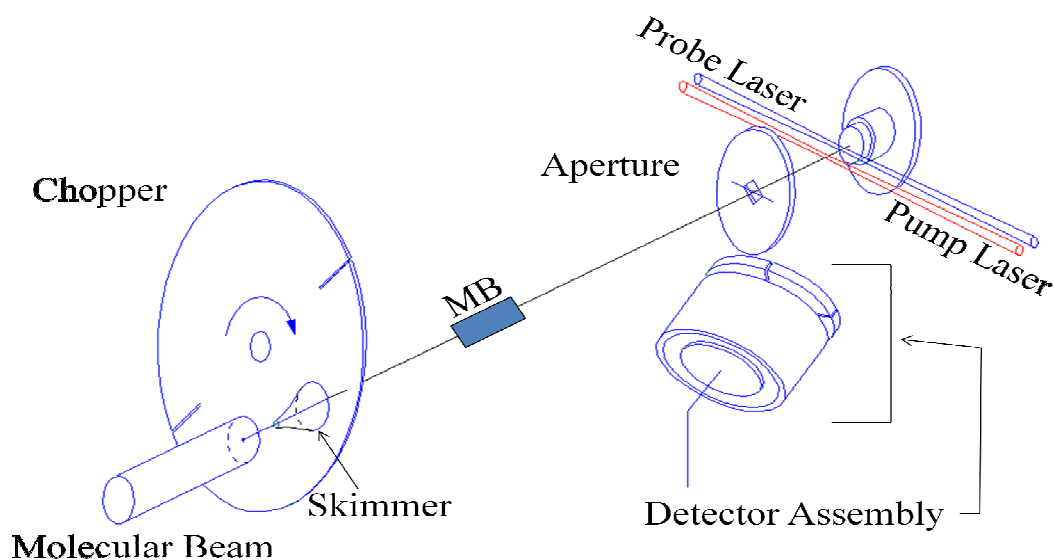


Fig. 2.1 General view of the experimental setup in the vacuum chamber

2.1 SAMPLE PREPARATION

The Cu (100) sample is 1 cm in diameter, held tight by two thin wires onto a stainless steel sample holder. The sample is heated from the rear by electron bombardment emitted from a 2% thoriated tungsten filament and is cooled conductively

using liquid nitrogen. The sample holder has a hole in the middle under the copper so the electrons directly hit the back of the copper sample. We want to measure Ar⁺ ion current hitting the sample during sputtering and the electron beam current hitting the sample during electron spectroscopy measurements and for this purpose the sample is electrically isolated from the rest of the sample manipulator. This is done by inserting a sapphire ring between the sample holder and the copper block where the liquid nitrogen flows through for cooling purposes. Other than electrical isolation the sapphire ring properties offer extra help. The thermal conductivity of sapphire increases when it is cold and so, when we cool the sample there is more heat transfer cooling the sample faster. The same property decreases at high temperatures thus decreasing the heat transfer from the sample to the liquid-nitrogen-temperature-cold copper block. Cleaning process includes 30 minutes of sputtering with 350 eV Ar⁺ ions while at 550°C and then annealing for another 30 minutes at 600°C. After the cleaning EELS, Auger electron spectroscopy (AES) and low energy electron diffraction (LEED) confirmed a clean copper surface with no contaminants and sharp LEED pattern. While AES and LEED are widely used as methods to monitor the surface cleanliness we have proven that EELS is far more sensitive to surface impurities than the other two. For the first time, surface cleanliness was monitored by measuring the intensity of the surface plasmon.

2.2 MAIN CHAMBER

Our experimental work is focused on the dynamics of molecules at surfaces. High background pressure changes the properties of the system, particularly the surface, in an uncontrollable way. We use low index single crystals and the purity of the sample surface

is essential for surface dynamics studies. The background residual gasses would stick on the surface with their respective sticking probabilities thus blocking the surface from the incoming molecules whose interaction we are interested in. High background pressure would reduce the beam flux by scattering. Thus we use pumps to maintain very low pressure: ultra high vacuum (UHV). The main residual gasses in a vacuum system are monitored by quadrupole mass spectrometer (QMS) are hydrogen ($m/e=2$), water ($m/e=18$), carbon monoxide and nitrogen ($m/e=28$), and carbon dioxide ($m/e=44$). The diffusive property of the gasses makes it difficult to maintain UHV. For example, hydrogen has a pressure up to 10^{-7} Torr inside the walls of the stainless steel made vacuum chamber. The low pressure in the main chamber (scattering chamber) is maintained by Varian V701 Turbo Molecular Pump. V701 is backed by a mechanical pump. Pneumatic valves and mechanical foreline valves are used to control the pumping. To reduce the partial pressures of residual gasses we cool a cylinder inside the chamber with liquid nitrogen. The cylinder is approximately 4 inch in diameter and 12 inch tall. When cold the total pressure in the chamber is lower than 2×10^{-10} Torr.

2.3 MOLECULAR BEAM PREPARATION

Supersonic molecular beams are used for surface-gas interaction studies because they provide a narrow velocity distribution. The usage of molecular beams has had its ups and downs and this was motivated, as it should be most of the time in science, by success of some and failure of others. After the unsuccessful attempt in working with molecular beams the famous Kistiakowsky assessed that “molecular beams are a graveyard for good chemists.” [26] After his inconclusive struggle in working with molecular beams he destroyed the apparatus with an ax [27].

The source chamber consists of two separately pumped vacuum chambers. The first contains the nozzle and the second the chopper wheel as shown schematically in Fig. 2.1. The source chamber, where the molecular beam is prepared, is pumped by Varian diffusion pump backed by mechanical pump. The pressure in the source chamber is approximately 1×10^{-8} Torr. When running the experiment the pressure increases to 6×10^{-6} Torr. The pressure in the buffer chamber, which is smaller in volume and houses the chopper, is 4×10^{-8} Torr and increases to 2×10^{-7} Torr when running the experiment. Molecules are brought from high purity hydrogen tank at 600 psi to a 20 psi pulsed nozzle. The nozzle temperature is changed from 25°C up to 500°C . A wire heats the front part of the stainless steel nozzle. The wire is electrically isolated from the nozzle by boron nitride. The temperature of the nozzle is measured using a K type Alumel-Chromel thermocouple which is spot-welded at the front of the nozzle. Cooling is done by water. After each nozzle pulse a beam expands in the source chamber, cools and becomes a supersonic beam. The nozzle opens 500 μsec each time 10 times a second thus is open only 5 milliseconds per second. A skimmer selects a very small part of the beam as it enters the buffer chamber.

The pulsed nozzle and the two lasers pumping and probing the beam are triggered by an optical signal from the chopper which rotates at 300 Hz. In the buffer chamber a chopper chops the most intense part of the beam in a direction perpendicular to the direction of propagation. The chopper is a thin rotating disc where slits are cut to allow only part of the molecular beam to pass by letting it pass through a slit 0.9 mm wide. The small slit allows the passage of molecules for only 6.5 μs and this is the main factor deciding the length of the molecular beam pulse. This chopped beam proceeds into the main chamber. At the entrance of the main chamber a horizontal wire, of width 0.38 mm,

cuts a slice from the cylindrical molecular beam thus creating a region where there are no molecules. (Wire cuts in half the cross-section of the beam perpendicular to the propagation direction. Use will be explained later.) The molecular beam size in the main chamber is approximately 2.5 cm long and 5 mm in diameter.

After entering the main chamber, the pump laser pumps a small part of the beam into a desired quantum state. To measure these incoming pumped molecules they are ionized by a probe laser. The ionized molecules are attracted by high negative voltages and are steered to the channel electron multiplier array (CEMA) ion detector. The molecules after passing the laser pumping and probing region hit the crystal surface. Depending on the sticking probability, a function depending on both the surface and the molecule, some of the molecules in the beam stick on the surface and stay. The other molecules are scattered back in a wider angle thus having a smaller density. To measure the scattered molecules the probe laser ionizes them. Time resolved spectroscopy requires all the devices to be synchronized.

2.4 PUMPING AND PROBING OF THE MOLECULAR BEAM USING OPTICAL METHODS

We are interested in studying quantum state resolved scattering of hydrogen molecules. The detection of specific states is achieved by (2+1) resonance enhanced multi-photon ionization (REMPI). Hydrogen molecules are excited by two photons in the ultra violet energy range from the $X^1 \Sigma_g^+$ ground electronic state to the $E, F^1 \Sigma_g^+$ via the Q-branch. 15.4 eV is the energy required to ionize a hydrogen molecule and the first two photons have given to the molecule an energy of approximately 12 eV. A third photon ionizes the molecule [28]. The photons should have wavelengths 201.75, 205.6 and

209.36 nm in order to ionize $H_2(v=0, J=1)$, $H_2(v=1, J=1)$ and $H_2(v=2, J=1)$ respectively. These photons are acquired through several steps. Originally we have a Nd^{3+} :YAG laser which outputs a 532 nm wavelength. This output is used to pump a tunable dye laser. The dye is Rhodamine 640 and its peak energy is at 603 nm and then drops somewhat linearly to zero at 630 nm. Then this light is passed through two nonlinear crystals: potassium dihydrogen phosphate (KDP) and β -barium borate (BBO). The first one doubles the frequency of the dye laser and these two frequencies, the fundamental and the doubled, are mixed in the BBO. The third harmonic of the fundamental is then focused onto the molecules inside the chamber perpendicular with respect to the molecular beam propagation. One shot of the laser ionizes only the molecules that are in an area the molecular beam viewed from the side equal to the focus area. The diameter of the laser focus spot is estimated to be 76 μm . The ions reach the CEMA and the signal is sent to a pre-amplifier and then read as a voltage by a computer. Each laser shot ionizes molecules in a new beam pulse. The molecular beam has a time-width of 8 μs at the position of the probe laser. Scanning of the probe laser in time gives a profile of MB and the peak arrival time at the position of the probe laser. This is along the direction of the MB and yields a time of flight measurement (TOF). Taking TOF data at several probe laser positions gives a set of beam positions and arrival times. By fitting these data the velocity and the translational energy of MB is determined. The translational energy of the beam is changed by heating of the nozzle. This way we can probe the ro-vibrational quantum states corresponding to the ground vibrational state only. Ro-vibrational states of $v=1$ have very small populations, even less are in the higher v -states. Only after heating the nozzle to temperatures higher than 600°C can we observe thermally populated, excited vibrational states. The ro-vibrational quantum states with $v=0$ are easy to detect since

they are highly populated. To study the dynamics of ro-vibrational states corresponding to $v=1$ we need to populate the MB with these states and this is achieved using a second laser, the pump laser. The pump laser is originally a 532 nm YAG beam that is enriched with Raman shifted frequencies as it passes through a Raman cell. The Raman cell is filled with the gas of interest, in our case hydrogen, to a pressure of around 30 psi. The fundamental 532 nm will be associated with the signatures of hydrogen intrastate transitions with the most intense being the ones that come from the most populated quantum state of hydrogen. So we expect intense shifted Raman light that corresponds to the transitions from ($v=0, J=1-5$) to the allowed states obeying the selective rules $\Delta v=+1$; $\Delta J=0, \pm 2$.

One goal of this work is to compare the translational energy exchange for scattering of ground and vibrationally excited H_2 from Cu (100). We measure the incident and scattered translational energy using a pulsed beam and time resolved laser spectroscopy. One experimental problem with making this comparison is the very different time scale for ground state measurements vs. those for the excited state. Typical TOF of ground and vibrationally excited state is shown in Fig. 2.3.i and 2.3.ii respectively. The width of the ground state pulse is 8 μsec and the peak time is determined with an error $\pm 0.5 \mu\text{sec}$ whereas for the excited state the pulse width is 0.1 μsec and peak time determined with an error of $\pm 0.01 \mu\text{sec}$. Thus, experimentally it is easier to determine translational energy with greater precision for the excited state when compared to the ground one. The reason is that in the 2.5 cm long MB the whole volume of the pulse has high population of ground state hydrogen molecules and experimentally-impossible-to-measure population of excited states. The excited states can be measured only when the pump laser is focused on the beam. So, for the excited state, in the 2.5 cm

long MB there is high population only in a region as big as the pump laser beam focus spot, $\approx 80 \mu\text{m}$ in diameter. Another problem that stresses the importance of precision is that when we measure the scattered molecules, both the ground and vibrational state, we measure TOF in a range 2.5 mm of probe positions in steps of 0.2 mm. For a $\Delta x = 0.2 \text{ mm}$ the change in arrival peak time is less than 0.1 μsec . This is not a problem for the excited state since the uncertainty is very small. The ground state having an uncertainty approximately five times larger than the time difference between two different TOF creates a problem.

This problem is solved by measuring the ground state in two steps. We first pump to the excited state using the pump laser and then probe with the probe laser. The way to measure TOF for the ground and excited state is shown schematically in Fig. 2.3. The pumped quantum states that we were interested in in this work is $(v=1, J=1)$.

To measure the incident translational energy of the ground state we do the following. The pump laser is focused on the molecular beam pumping the molecules from $(v=0, J=1)$ to $(v=1, J=1)$. The pump and the probe, have to be carefully aligned with respect to each-other. These pumped molecules, occupying a tiny region in space, are probed (ionized using the quantum-state-corresponding REMPI wavelength) using the UV light. Unlike probing the 2.5 cm long beam as explained above, with the two laser experiment we probe molecules that are in a spot with diameter equal to the pump laser focus size. The pumped molecules will “pass” in front of the probe laser in approximately 60 nsec. We measured TOF spectra for the excited state by scanning the probe laser firing time in steps of 10 nsec. The velocity of the molecules does not change when they are pumped. To measure the scattered translational energy we pump the $(v=0, J=1)$ molecules as they scatter very close to the sample. Then the pumped molecules having

the same KE as the ground state are measured with the probe laser. The incident and the scattered translational energy of the ($v=1, J=1$) excited state is measured simultaneously. The pump laser pumps molecules to ($v=1, J=1$) state and the probe laser is scanned for a longer time thus measuring the incident molecules and the scattered ones. In Fig. 2.3.iii it can be seen that the width of TOF is larger than for Fig 2.3.ii.

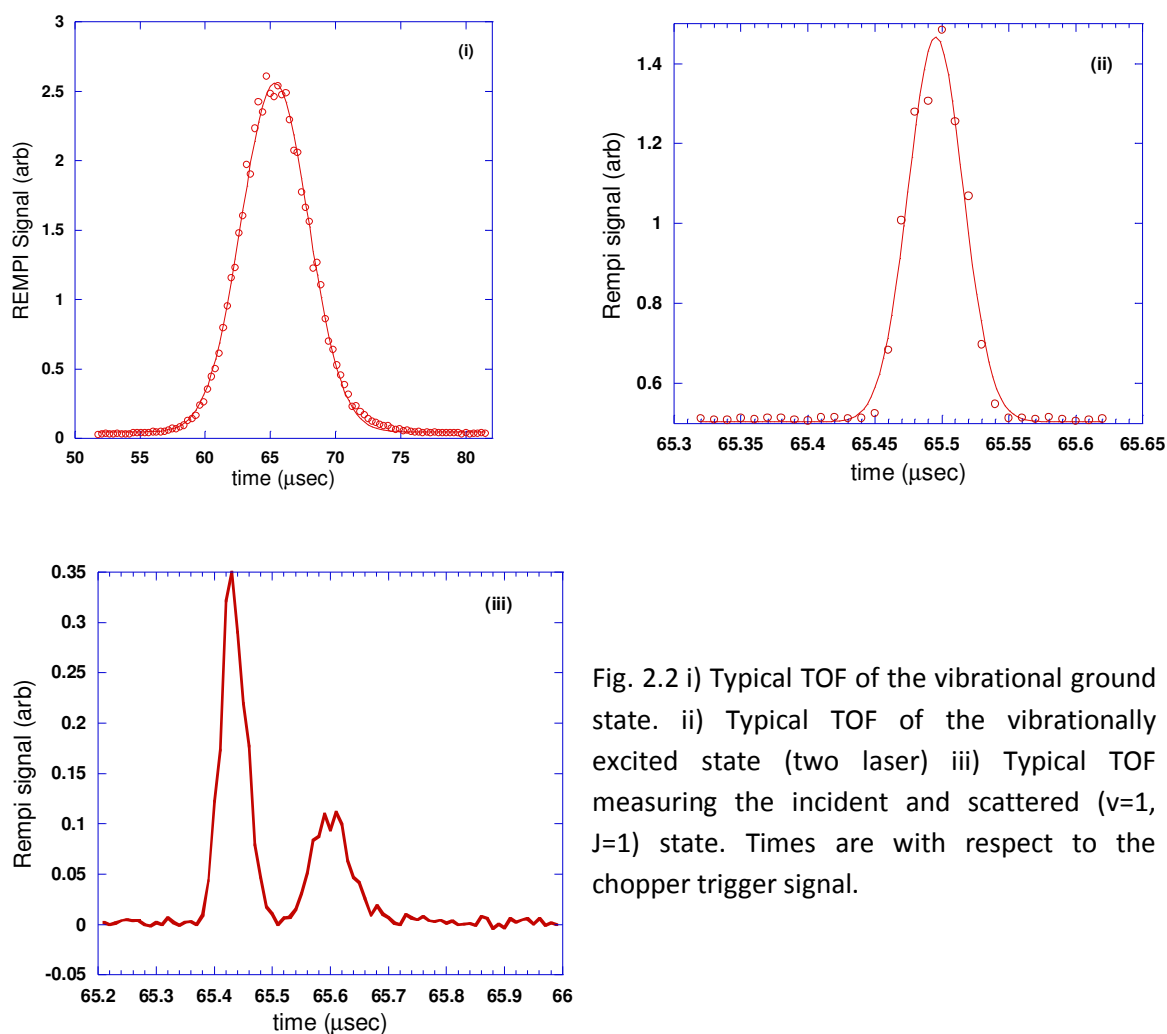


Fig. 2.2 i) Typical TOF of the vibrational ground state. ii) Typical TOF of the vibrationally excited state (two laser) iii) Typical TOF measuring the incident and scattered ($v=1, J=1$) state. Times are with respect to the chopper trigger signal.

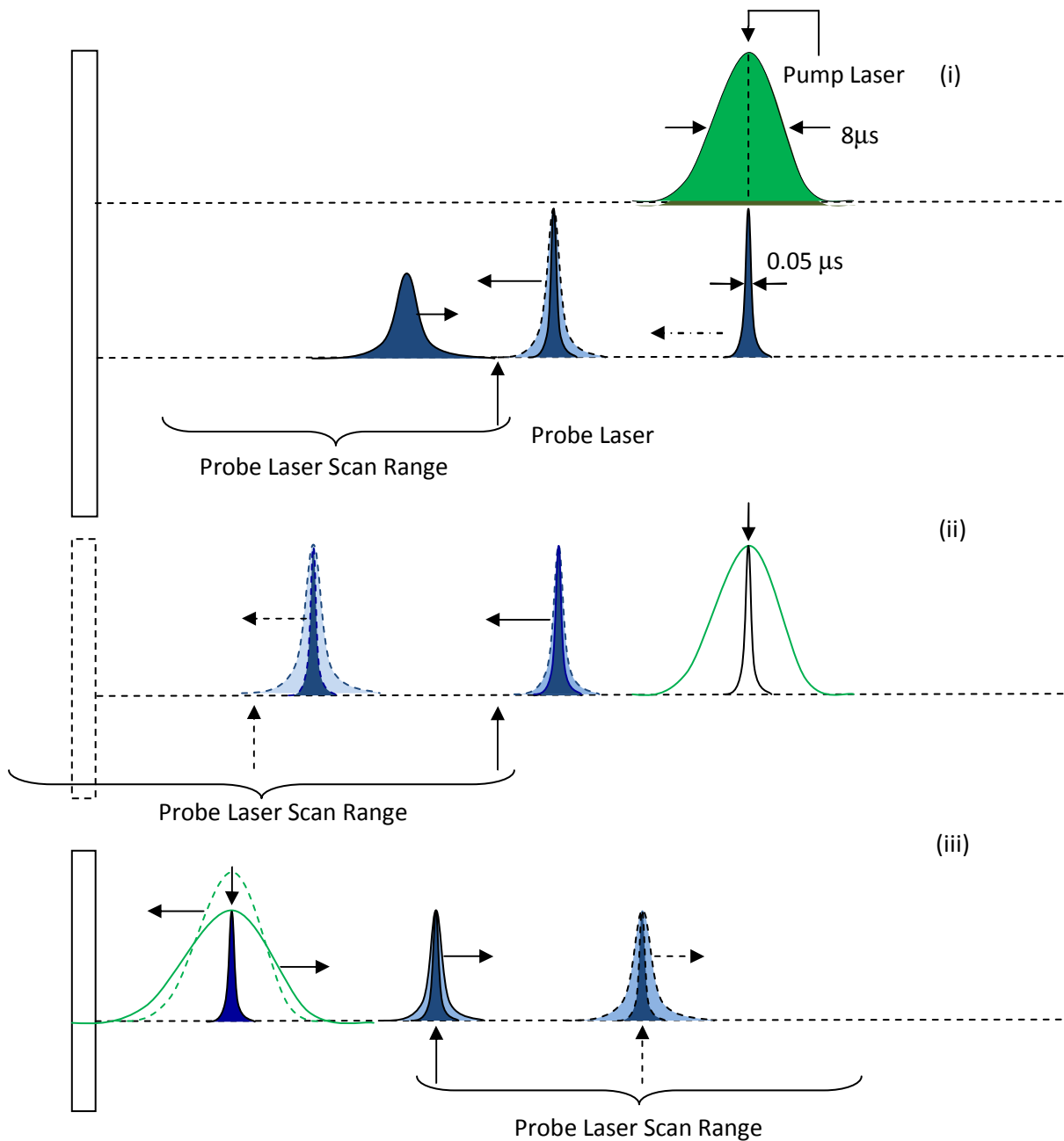


Fig. 2.3 (i) Measurement of initial and scattered energy for $(v=1, J=1)$. The MB is pumped and then probed by the probe laser which ionizes them. One TOF is $\approx 1\mu\text{s}$ wide in order to ionize the scattered signal too. (ii) Measurement of the incident energy of $(v=0, J=1)$. MB is pumped from $(v=0, J=1)$ to $(v=1, J=1)$ at the peak time and the pumped pulse is probed by probe laser. Sample is taken out of the MB path. (iii) Measurement of the energy of the scattered $(v=0, J=1)$. $(v=0, J=1)$ is pumped and then is probed by the probe laser. Note that in all cases the probe laser is set at corresponding ionizing wavelength of $(v=1, J=1)$.

We have to be careful with the probe laser and try to keep it from scattering from the sample because the UV photons would eject electrons that would saturate the CEMA. Another reason to keep both lasers away from the sample is that the sample could get dirty. The laser beam has a waist width at the focused point so it is difficult to find sample position using the laser. With the UV laser though we can “precisely” scan the wires of the sample holder giving us confidence about the focusing of the laser and also on the possibility of scanning different molecules when we change probe laser position by very small distances. Another supporting argument of this is that using the probe laser we can find the region that is sliced/cut out by the horizontal wire at the entrance of the main chamber. The diameter of the wire is 0.38 mm thus the shadow (region where there are no molecules) should be the same, ideally. Measured by the probe laser the shadow is 0.3 mm. So the size of the laser focus is 80 μm .

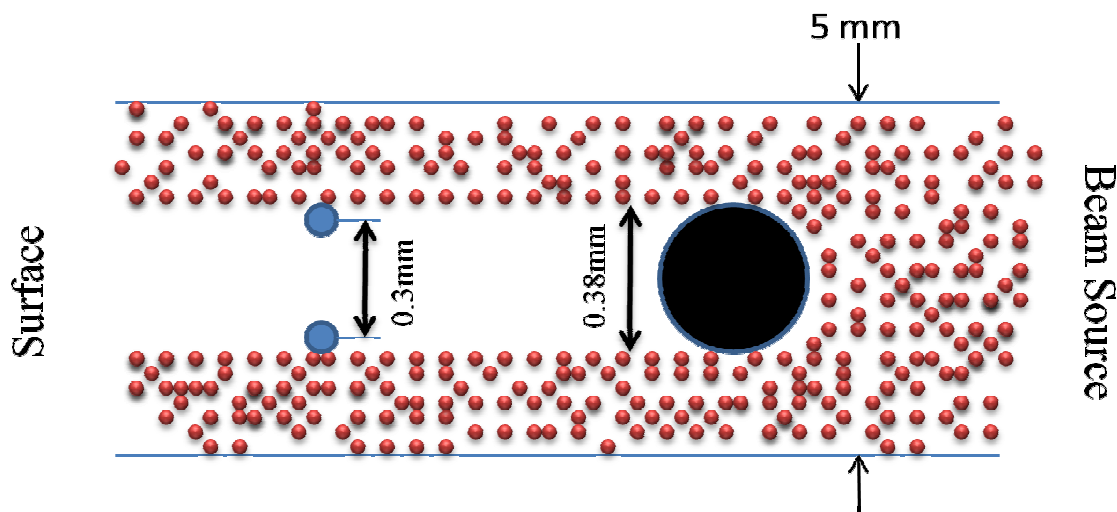


Fig. 2.4 The shadow created by the wire is shown (Diam.=0.38mm) The blue small circles represent the probe laser. The drawing is not to scale.

2.5 ELECTRON SPECTROMETER

Cu(100) is studied using electron spectroscopy. Using a reverse view LEED (low energy electron diffraction) apparatus, Auger electron spectroscopy (AES), electron energy loss spectroscopy (EELS) and virtual temperature programmed desorption (VTPD) measurements were performed.

LEED is very sensitive to the surface atomic arrangement. Electrons of energies 20-330 eV are emitted from the electron gun and hit the surface at normal incidence. The De Broglie wavelength of the electron is a few angstroms, less than 3 Å, thus it scatters from atomic lattices. Pattern of the reciprocal lattice (not to scale) are created on a phosphorus fluorescent screen. A general schematic is shown in Fig 2.5. Programmed voltages on the inner grids G2 and G3 (we will call it G23) allow only diffracted electrons that have enough energy. The same apparatus is used for AES and EELS. This time the voltage at the G23 has been adjusted. The voltage acting as a bias is a DC voltage with a 400 Hz AC component added on. The signal collected and measured is the total number of the electrons reaching the screen with an energy larger than bias voltage at the G23. The measured signal is sent to a lock-in-amplifier. The lock-in amplifier takes the first derivative of the signal and that gives the number of the scattered electrons at a certain energy interval, ΔE . This is how EELS data is taken. The EELS signal is in a range 5-30 eV less than the incident electron beam energy. The backscattered electrons have lost this energy by exciting an oscillation of the electron gas called a plasmon. An example of EELS is shown in Fig 2.6.

The Auger electron energy is not a function of incident electron beam energy. Yet the energy of the electrons in the beam should be larger than sum of the binding energy and the work function. The energy (kinetic energy) of the emitted electrons is a signature

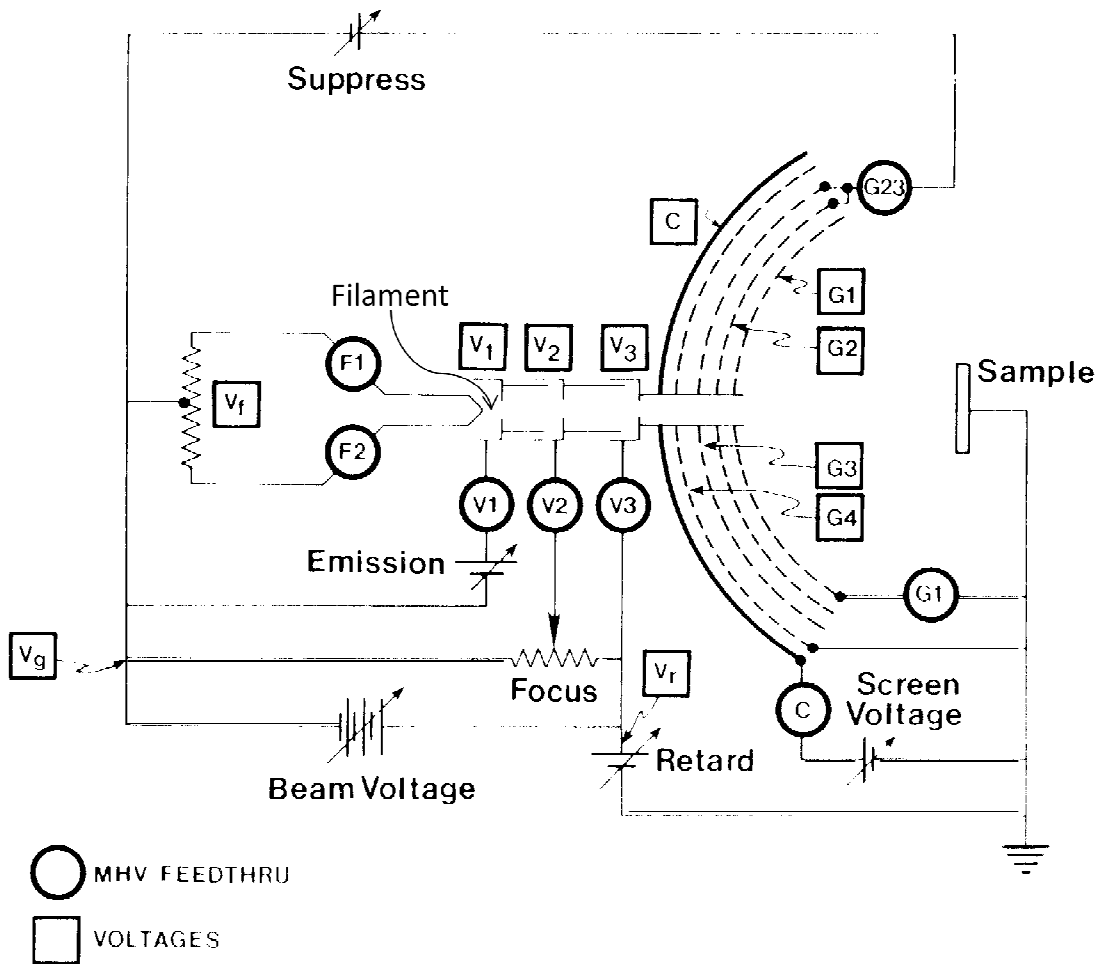


Fig. 2.5 General schematics of LEED apparatus and required electrical connections. [29]

of an inner transition of an electron from an outer level to an inner one. A high energy electron comes, hits an inner shell electron and forces it to leave the atom. Electrons from the outer shells will fall into vacancy level and the energy difference between the outer shell and the vacancy is given to another electron which is emitted with an energy

characteristic of the atom which now is double ionized. The energy region of the Auger electrons has a very high background and to make the detection easier the derivative of the EELS is taken. An Auger electron spectrum of copper is shown in Fig. 2.7.

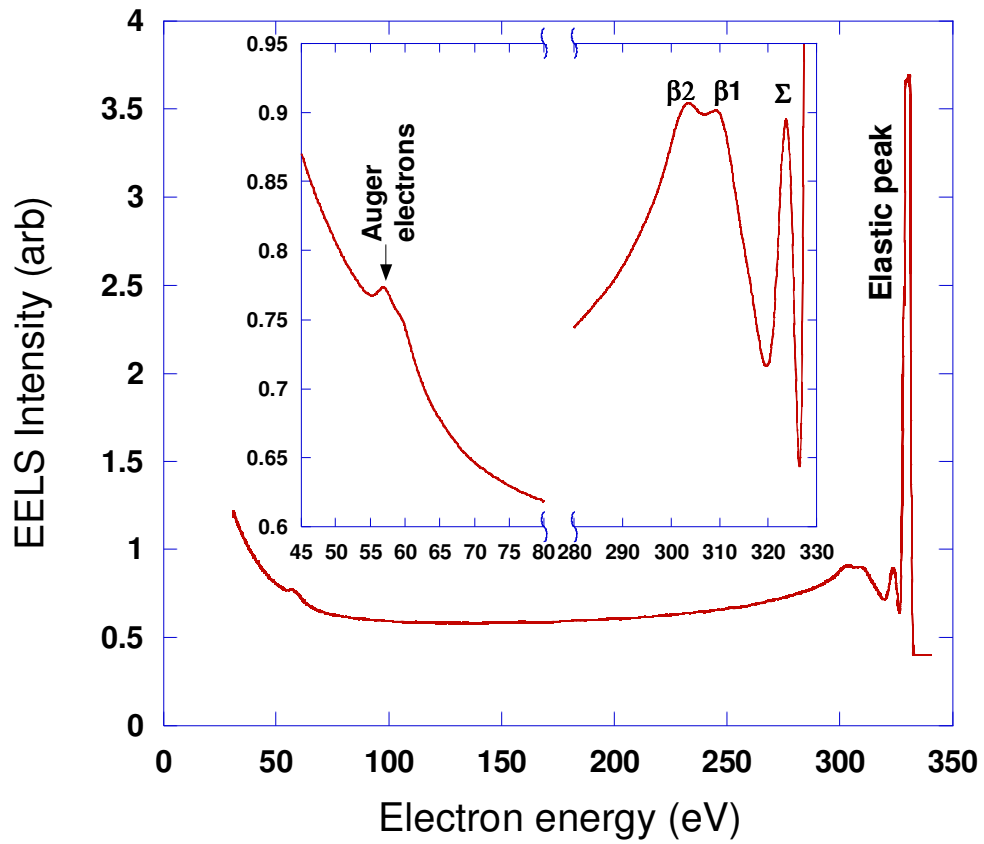


Fig 2.6 EELS measurement of copper sample. Energy of the incident beam is 330 eV. Inset shows surface plasmon (Σ), bulk plasmons (β_1 , β_2) and Auger electrons (58 eV).

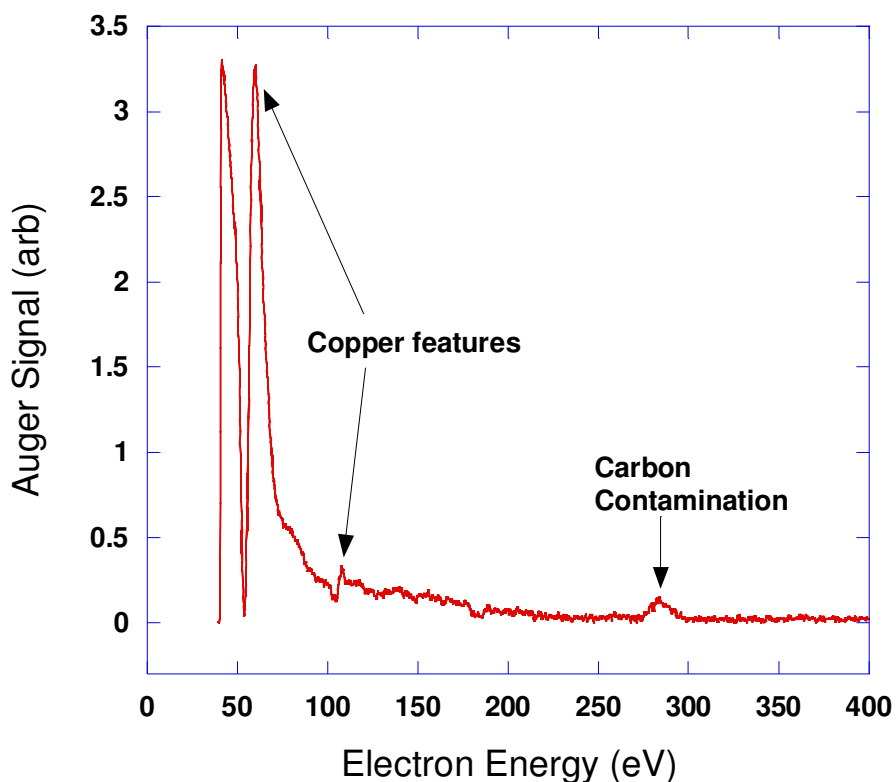


Fig. 2.7 Auger measurement of copper sample before cleaning. Copper features are seen at 58 and at 105 eV. Carbon contamination is seen at 270 eV.

Temperature programmed desorption (TPD) is a widely used method to study surface adsorbates. The surface is heated and the desorbed molecules are monitored by a mass spectrometer. We performed TPD virtually (VTPD) by heating the sample but the monitoring was done by measuring the intensity of the surface plasmon. Intensity is smaller when the surface is covered and as heated the plasmon intensity increases to the value corresponding to that of a clean surface. The derivative of the intensity gives the VTPD. Heating is done at a constant rate thus the derivative can be considered to be with

respect to either time or temperature. A sample of such a measurement is shown in Fig. 2.8.

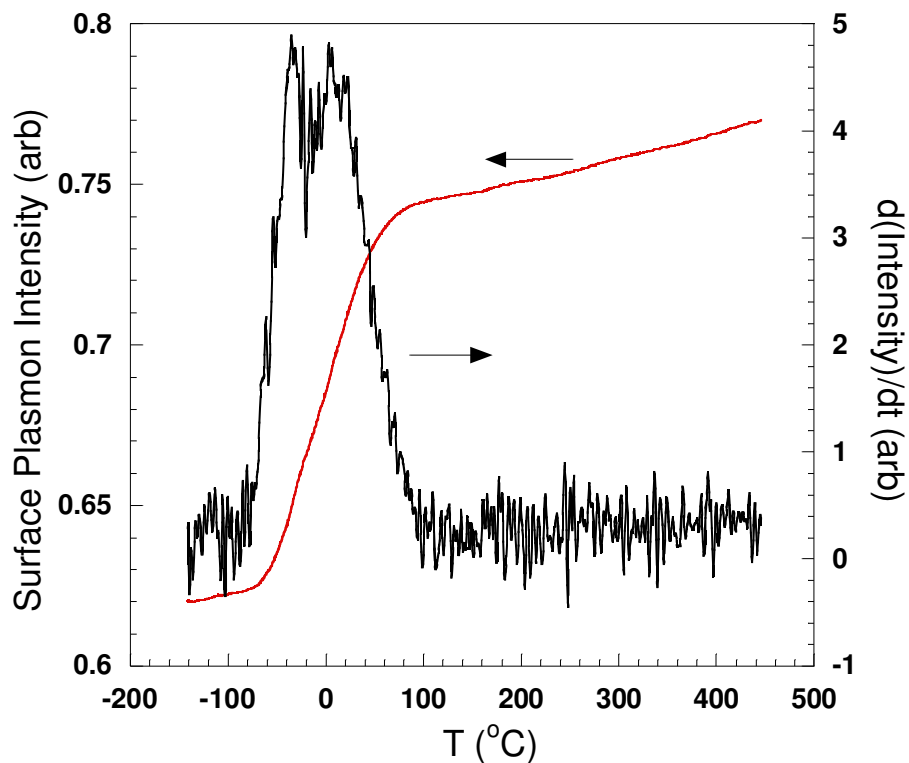


Fig. 2.8 Virtual TPD (VTPD) of H/Cu(100). Intensity of the surface plasmon and its derivative is shown. The derivative is proportional to the rate of desorption. $T = \beta x t$ (Heating rate is constant)

Chapter 3 Quantum State Resolved of H₂ Scattering from Cu (100)

A great deal of work both experimentally and theoretically has been done to study the dynamics of gasses close to the surface of metals and their interaction during adsorption, desorption and scattering. In the whole spectrum of molecule surface interactions there are some systems that serve as benchmarks and the two most studied have the molecule in common: H₂. These two referred systems are H₂/Cu for activated and H₂/Pd for the non-activated processes.

While there is a plethora of results for H₂ interacting with copper surfaces flowing in from both theory and experiments, we still do not have a complete understanding of the system because some of these results conflict with each-other. For example, the experimental work of Watts et al. proved that theoretical calculations overestimate the probability for rotational excitation of ($v=1, J=1$) into ($v=1, J=3$) upon scattering from Cu(100) [30, 31]. The pattern of results coming in for these two systems too have the same problem mentioned above, but many researchers believe that some of the conclusions for H₂/Cu and H₂/Pd may be of general validity. [32]

3.1 BACKGROUND WORK

One of the most interesting aspects of gas-surface interactions is the energy transfer between the degrees of freedom of the surface and the gas molecule. This includes translational, vibrational and rotational energy of the gas molecules as well as the energy

of the nuclei and electrons of the material composing the surface. Using state and time resolved spectroscopic techniques (REMPI and TOF) we can measure the energies in each of the gas-molecule DOF. The same cannot be said quantitatively for the energy changes in the substrate's DOF. The two possible pathways for energy transfer to the substrate are transfer from the phonons (exciting or deexciting a phonon) and the excitation of an electron into creating an electron-hole pair. While hydrogen is not expected to efficiently excite a phonon, electron excitation has been a subject of long and still unresolved debate.

All of the calculations modeling molecule-surface interaction involve some approximations. Many of them freeze the DOF of the substrate. Some consider reduced freedom for the molecules such as fixing the angle θ thus keeping the molecular orientation fixed as it stays parallel to the surface. Many use the adiabatic or Born-Oppenheimer approximation. In Born-Oppenheimer approximation the electrons are assumed to be in ground state all the time. The reasoning goes as follows: the electrons are much lighter than the nuclei and as the nuclei move the electrons, like all physical systems, trying to stay in the lowest energy level, can rearrange fast enough so that they stay in the ground state all the time. One may think of two possible situations where the adiabatic approximation could fail. One would be a situation where the nuclei, in the case of substrate-adsorbate system the nuclei of both of these, are moving very fast so that the electrons do not have time to rearrange to their lowest energy level. Another would be when the wavefunction of one electron of the incoming molecule overlaps with the wavefunction of the electrons on the substrate and so the electron on the substrate would move above the Fermi level with the energy taken from the incoming molecule.

These two possible cases were thought to be the possible situations when non-adiabatic effects show up but recent experimental work by Nahler *et al.* shows dependence on the inverse velocity of the incoming molecule of nonadiabatic effects. According to their model, which should be considered by theoreticians, the nonadiabatic electronic excitations observed are not due to the velocity of the molecule relative to the surface but the motion of the atoms in the molecule relative to each-other [19]. Their system was vibrationally excited NO scattered from Cs capped Au(111). The hydrogen molecule wavefunction can overlap with the wavefunction of the electrons on the surface for any distance smaller than about 3 Å, while for NO it is reported that the overlapping of the adsorbate-substrate electron wavefunction [19] starts for distances < 10Å.

The experimental methods used to measure the possible energy transfer channels have been developed extensively over the past 25 years. In early work infrared spectroscopy was used to resolve the natural linewidth of vibrational resonances of adsorbed species on metal surfaces and the first results suggested that the broadening of the linewidth was dominated by the energy transfer to the electron-hole pairs. [16] These early experimental studies that showed a channel of energy transfer between the adsorbed molecules and the substrate attracted the attention of theorists and in one of the earliest calculations by Brivio and Grimley [33] it was reported that energy loss to the electron system could be an important mechanism for sticking. The first *ab initio* calculations were reported by Persson and Hellsing [16] who showed that the effect of electron damping on the vibration of hydrogen chemisorbed on metals was important. These were the first hints of a coupling between the adsorbate and the electron excitations.

There have been many studies on the dependence of surface interactions on different DOF [34, 35]. Michelsen et al. [34] reported that translational and vibrational

energy affect the adsorption probability of hydrogen on copper with the former one being twice as effective. Smith et al. [36] examined the reactivity of methane on a nickel surface and found that vibrational energy is more effective than translational energy in promoting reactivity for some vibrational modes. The general idea is that the translational energy would largely affect adsorption and surface reactivity if the system has an early barrier (closer to the entrance) and the vibrational energy would affect if the case of a late barrier (closer to the exit). An example of the latter case is shown in Fig. 1.1.

3.2 EXPERIMENTAL RESULTS

In an effort to understand the mechanism involved during the scattering of hydrogen off of copper we measured the translational energy exchange of the vibrational ground and excited state during scattering. We took the data as explained in the experimental section. We measured the energy loss upon elastic scattering of the ($v=0, J=1$) and ($v=1, J=1$) quantum states at two surface temperatures as a function of incident energy in an attempt to understand the dependence of the energy loss on E_{inc} for the two mentioned ro-vibrational states of hydrogen. First data (of this kind) were taken by Jonghyuk Kim in our lab [37].

A typical set of data looks like the one shown in Fig. 3.1 where peak times of the TOF as a function of the probe laser position are shown for the incident and scattered molecules. From the data shown in Fig. 3.1 we can calculate the velocity of the incident and scattered beam and then the change in the kinetic energy of the beam. The sample

position with respect to the laser is determined from this data by the point where the incident and scattered curves cross ($b=17.3\text{mm}$ for the data shown).

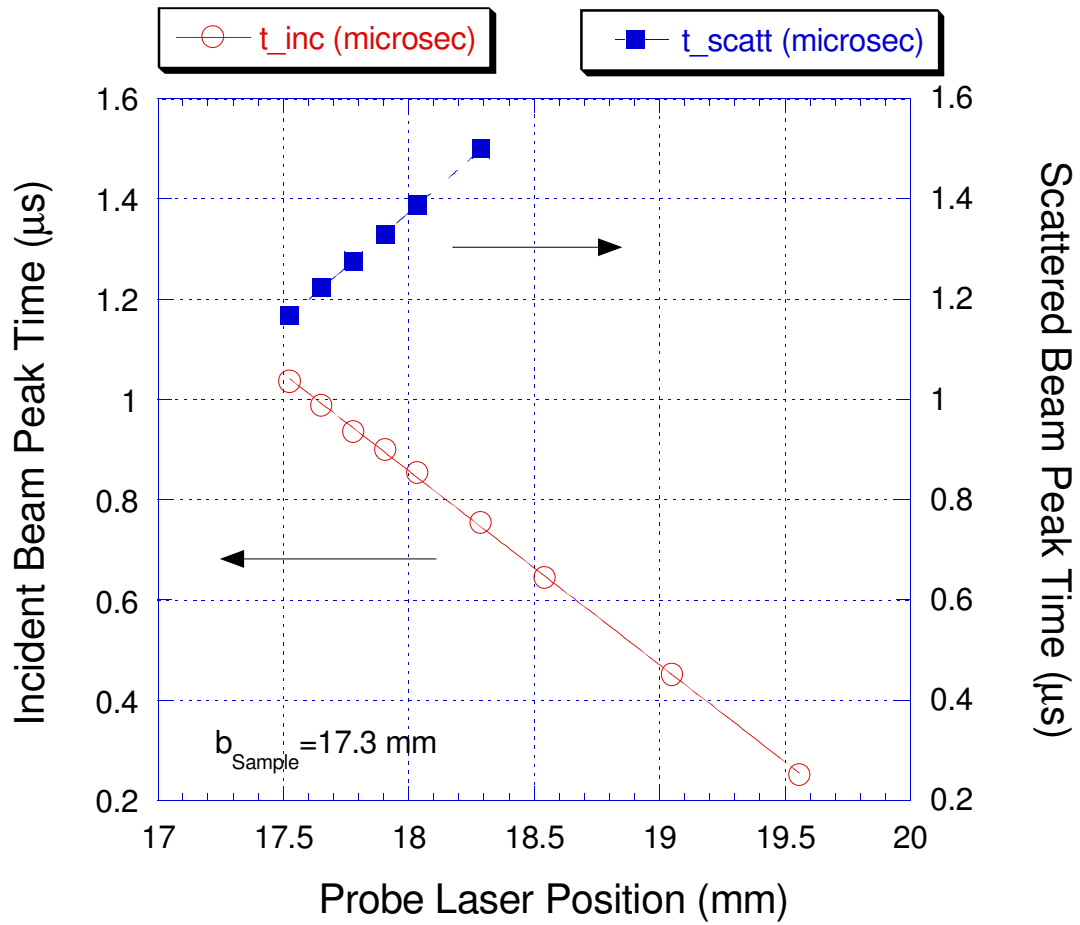


Fig. 3.1 Peak times as a function of probe laser position. From this graph we can calculate the velocity of the incident and scattered beam, change in the kinetic energy of the beam and the distance of the sample with respect to the laser.

In Fig. 3.2 we have plotted the scattered beam energy as a function of the incident one for two ro-vibrational states as they scatter from Cu(100) at 173 K and the detailed data is in Table 3.1. We find that the ground state loses slightly more energy than the excited one. If we consider the molecule-surface system classically where upon scattering the energy and the momentum have to be conserved we can use the Baule Equation to make a simple estimate of the energy loss [38]:

$$\Delta E(E_{inc}, T_{Cu}) = \frac{4\mu}{(1+\mu)^2} \left[E_{inc} - \frac{1}{2} k_B T_{Cu} \right] \quad \text{Eqn. 3.1}$$

where E_{inc} is the incident translational energy of the hydrogen molecule, k_B is the Boltzman constant ($k_B = 8.617 \times 10^{-2} \frac{meV}{K}$), T_{Cu} is the temperature of the copper surface and μ is the ratio of hydrogen molecule to the mass of one copper atom times the number of copper atoms that the molecule is interacting during the collision, $\frac{M_{H_2}}{nM_{Cu}}$ and n is the effective number of copper atoms that the hydrogen molecule exchanges energy with. In our measurement we changed only the incident energy of the hydrogen beam and so we expect a linear dependence of the energy loss as a function of E_{inc} , assuming n is not a function of E_{inc} .

From Fig 3.2 we can see a close-to-linear dependence of the scattered energy on the incident one for energies smaller than 150 meV for the vibrationally excited state and smaller than 125 meV for the vibrational ground state. We fitted the data in Fig. 3.2 to the Baule Equation in the range of energies smaller than 150 meV for the excited state and smaller than 125 meV for the ground state and we obtained $n=0.7$ and $n=0.5$ respectively. So the vibrationally excited hydrogen molecules are exchanging energy with a mass of

0.7 masses of copper atoms and the ground (unexcited) state with a mass of 0.5 masses of copper atoms.

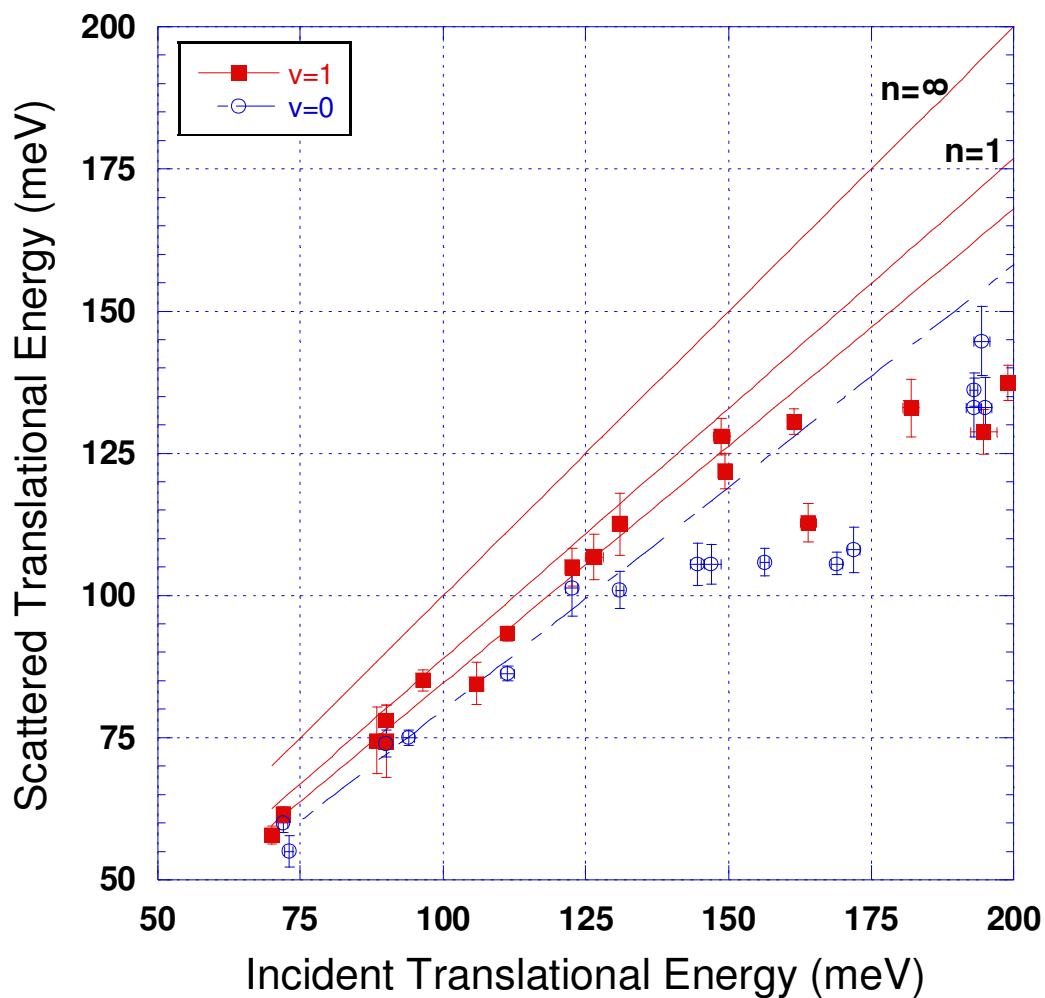


Fig. 3.2 Incident and scattered energy for H_2 ($v=0, J=1$) and ($v=1, J=1$) quantum states of hydrogen upon scattering from $Cu(100)$, $T_{Cu}=173K$. The lines are fits to the Baule equation in the low energy region where the data shows close to linear dependence. For comparison the energy exchanged for H_2 scattering from one copper atom ($n=1$) and an infinite mass atom ($n=\infty$) are shown.

Surface at 173K					
$H_2(v = 1, J = 1)$			$H_2(v = 0, J = 1)$		
Incident Energy (meV)	Scattered Energy (meV)	Energy Loss (meV)	Incident Energy (meV)	Scattered Energy (meV)	Energy Loss (meV)
72±0.8	61.6±1.2	10.4±1.2	72.0±0.8	60.0±1.7	12±2.5
88.5±1.1	74.5±5.9	14.0±7.0	73±0.8	55±2.8	18±3.6
90.0±1.0	78.0±2.7	12.0±3.7	90.0±1.0	74.0±2.4	16±3.4
96.5±1.1	85.1±1.9	11.4±3.0	94.0±1.0	75±1.4	19±2.4
105.8±0.6	84.5±3.7	21.3±4.3	111.3±1.2	86.3±1.3	25±2.5
111.3±1.2	93.3±1.3	18.0±2.5	122.6±1.1	101.3±4.9	21.3±6.0
122.6±1.1	105.0±3.3	17.6±4.4	131.0±0.7	101.0±3.3	30.0±4.0
126.5±1.5	106.8±4.0	19.7±5.5	144.6±1.3	105.5±3.7	39.1±5.0
131.0±0.7	112.6±5.5	18.4±6.2	156.4±0.8	105.9±2.4	50.5±3.2
148.8±1.4	128.0±3.2	20.8±4.6	169.0±1.0	105.6±2.0	63.4±3.0
149.4±0.9	121.9±3.1	27.5±4.0	172.0±1.1	108.0±3.9	64.0±5.0
161.5±1.1	130.6±2.2	30.9±3.3	193.0±1.3	133.0±5.2	60.0±6.5
164.0±1.4	112.8±3.4	51.2±4.8	193.0±0.7	136.2±3.0	56.8±3.7
182.0±1.4	133.0±5.1	49.0±6.5	194.4±1.4	144.7±6.1	49.7±7.5
194.7±2.3	128.8±3.9	65.9±6.2	195.0±1.1	133.0±5.4	62.0±6.5
199.0±0.7	137.4±3.1	61.6±3.8			

Table 3.1 Translational energy loss for $H_2(v=1, J=1)$ and $H_2(v=0, J=1)$ upon scattering from Cu(100) surface at 173K.

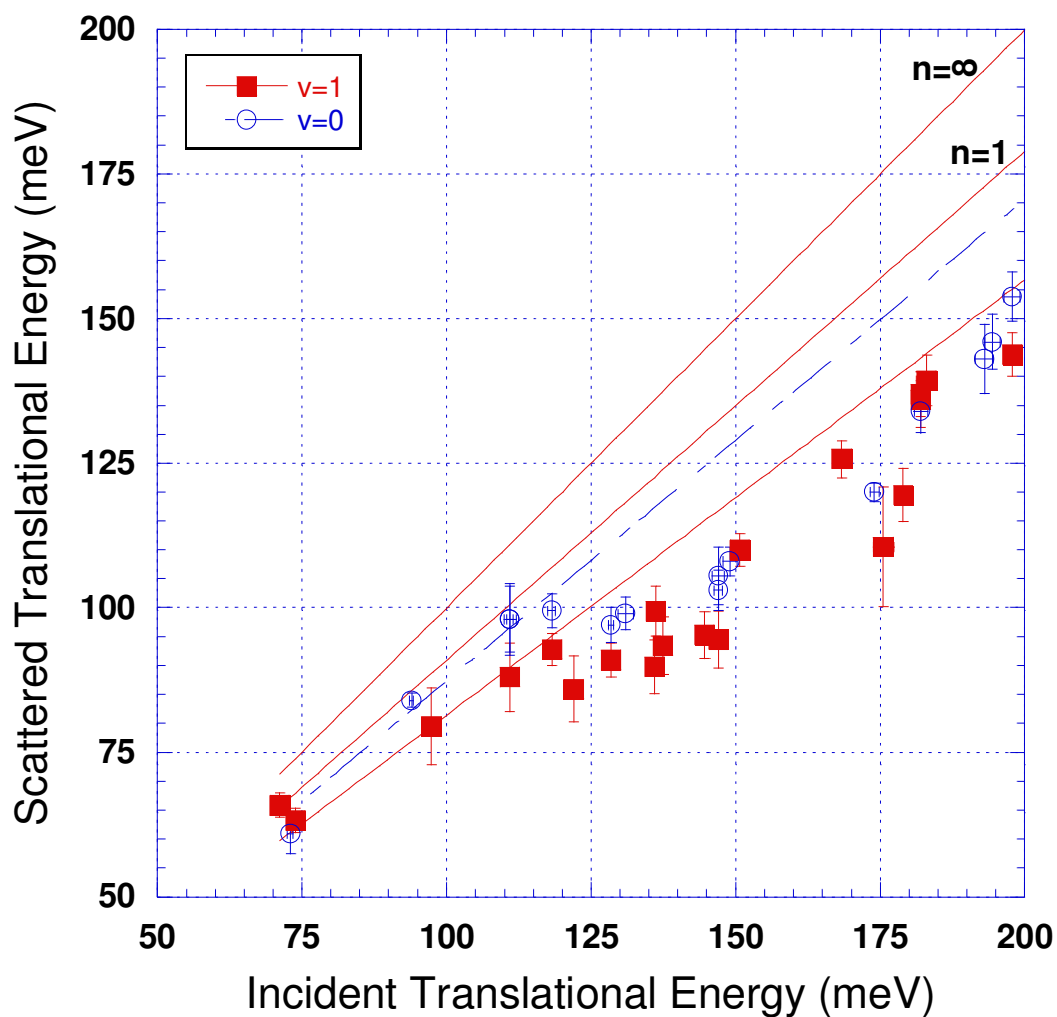


Fig. 3.3 Incident and scattered energy for H_2 ($v=1, J=1$) and H_2 ($v=0, J=1$) quantum states of hydrogen upon scattering from Cu(100), $T_{Cu} = 573$ K. Data is fitted to the Baule Eqn. in the low energy range. $n_{(v=1, J=1)}=0.5$, $n_{(v=0, J=1)}=0.7$. For comparison the energy exchanged for H_2 scattering from one copper atom ($n=1$) and an infinite mass atom ($n=\infty$) are shown.

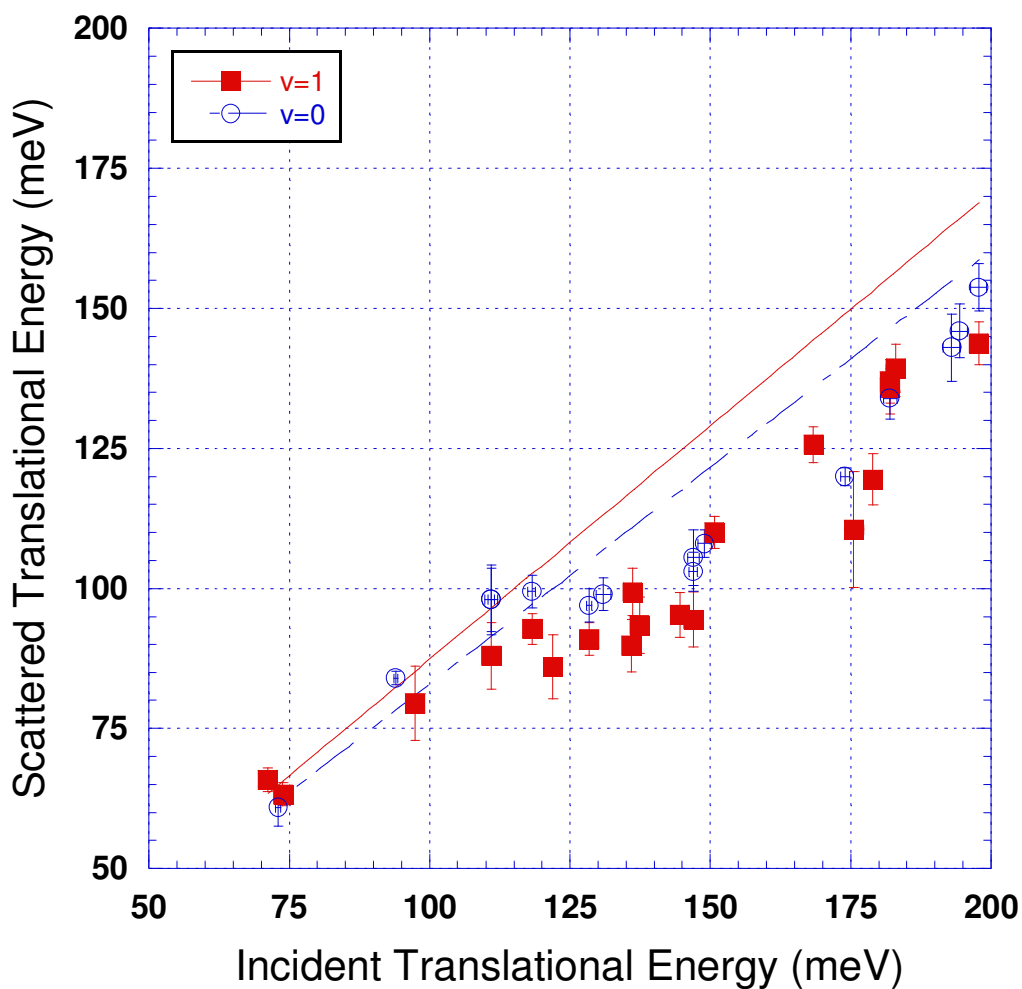


Fig. 3.4 Incident and scattered energy for H_2 ($v=1, J=1$) and H_2 ($v=0, J=1$) quantum states of hydrogen upon scattering from Cu(100), $T_{Cu}=573K$. Data is fitted to the Baule Eqn using n -values found for the cold sample.

In Fig 3.3 and Table 3.2 we show similar data for a surface temperature of 573K. The general trend that we observe here is that the vibrationally excited state loses slightly more energy than the vibrational ground state. The Baule fits yield $n_{(v=1, J=1)}=0.5$ and $n_{(v=0, J=1)}=0.7$.

<i>Cu(100)</i> Surface at 573K					
$H_2(v = 1, J = 1)$			$H_2(v = 0, J = 1)$		
Incident Energy (meV)	Scattered Energy (meV)	Energy Loss (meV)	Incident Energy (meV)	Scattered Energy (meV)	Energy Loss (meV)
71.2±0.3	65.9±2.1	5.3±2.4	73.0±0.5	61.0±3.5	12.0±4.0
73.9±0.4	63.2±2.1	10.7±2.5	94.0±0.3	84.0±1.2	10.0±1.5
97.4±1.0	79.5±6.7	17.9±7.7	111.0±1.1	98.0±5.7	13.0±6.8
111.0±1.1	88.0±5.9	23.0±7.0	118.2±0.7	99.5±2.9	18.7±3.6
118.2±0.7	92.8±2.8	25.4±3.5	128.5±0.4	97.0±3.0	31.5±3.4
122.0±0.9	86.0±5.7	36.0±6.6	131.0±1.3	99.0±2.9	32.0±4.2
128.5±0.4	91.0±2.9	37.5±3.3	147.0±0.7	103.0±3.5	44.0±4.2
136.0±1.2	89.8±4.7	46.2±5.9	147.0±1.0	105.5±4.9	41.5±5.9
136.1±1.4	99.4±4.3	36.7±5.7	149.0±1.2	108.0±2.4	41.0±3.6
137.4±1.1	93.5±5.0	43.9±6.1	174.0±0.8	120.0±1.6	54.0±2.4
144.6±1.2	95.3±4.0	49.3±5.2	182.0±1.2	134.0±3.8	48.0±5.0
147.0±1.4	94.5±4.9	52.5±6.3	193.0±1.5	143.0±6.0	50.0±7.5
150.7±1.2	110.0±2.8	40.7±4.0	194.4±1.3	146.0±4.7	48.4±6.0
168.4±0.8	125.7±3.2	42.7±4.0	197.8±1.4	153.8±4.2	44.0±5.6
175.6±1.7	110.5±10.3	65.1±12.0			
179.0±1.2	119.5±4.6	59.5±5.8			
182.0±0.7	136.0±4.8	46.0±5.5			
182.0±1.1	137.0±3.9	45.0±5.0			
183.0±1.7	139.3±4.3	43.7±6.0			
197.8±1.4	143.8±3.8	54.0±5.2			

Table 3.2 Translational energy loss for ($v=1, J=1$) H_2 and ($v=0, J=1$) H_2 upon scattering from $Cu(100)$ surface at 573K.

Understanding the relative contribution of the kinetic and vibrational energy in the reaction probability and the nature of the reaction have been long standing goals. Our work tries to answer two questions: i) what is the relative importance of vibrational energy and translational energy?, ii) is the scattering adiabatic or non-adiabatic?

Theoretical and experimental evidence has been found supporting both possibilities when trying to resolve the first question (the relative effectiveness of KE vs vibrational energy). There is a set of experiments that have concluded that for certain systems vibrational energy is more effective in promoting reaction [36] and energy transfer [19]. Smith et al. observed that reaction probability increases with vibrational energy for the CH₄/nickel system. The work of Nahler et al. proved that energy exchange is inversely dependent on velocity, contradicting the idea of translational energy dominance. Katz et al. had previously predicted the opposite using a non-adiabatic model [39]. Together with these results there is another set of work done by different groups for H₂-copper system where translational energy is proven to be more efficient than vibrational energy in promoting reaction probability. Anger et al. [40] have reproduced experimentally measured sticking probabilities by modeling them as functions of kinetic energy only and Michelsen et al. reported that despite the coupling of the vibrational and rotational motion to the reaction coordinate the translational energy is by far the most effective in assisting the molecule over the barrier to adsorption [34].

More interesting has been the discussion of the second question of whether the reaction is adiabatic or not. The whole idea of nonadiabatic effects has been discussed for some time [25, 41-43]. The work of Nieto et al [41] and by Juaristi et al. [42] brought the adiabatic approximation back to life. Luntz and his coworkers support the importance of nonadiabatic effects on molecule-surface system and have been critical of the

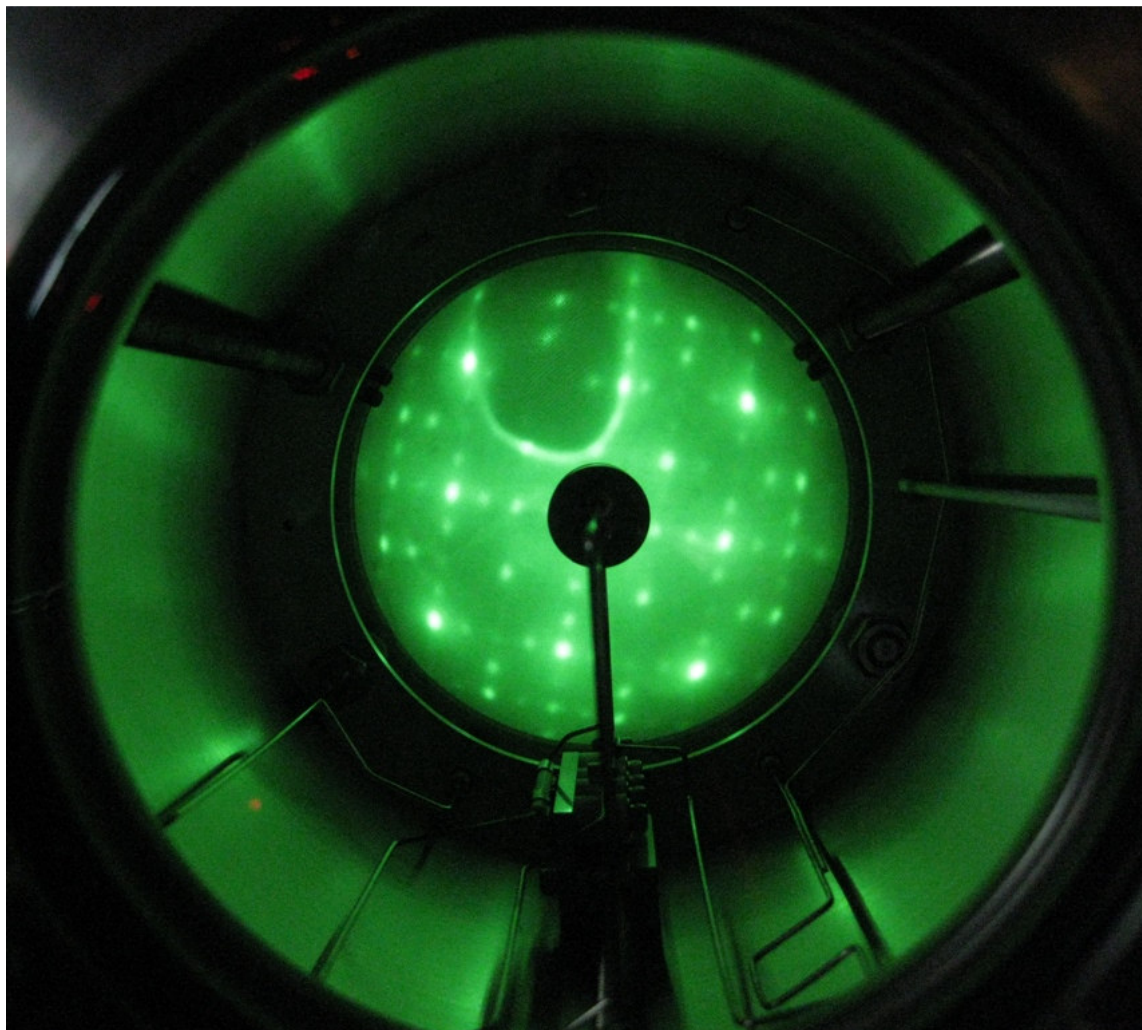
approximations used in the theoretical calculations of Juaristi and coworkers. Nieto et al. claimed that their calculations for H_2/Pt (111) supports the conclusion that reactive and nonreactive scattering of H_2 from a metal surface is electronically adiabatic [41]. For the same system part of the molecules may exchange energy through nonadiabatic channels and part may not. It is difficult to say that all the molecules undergo adiabatic or nonadiabatic processes since this probability of undergoing either one of the processes may be the deciding factor in the reaction probability (some molecules may stick on a surface and some may scatter and this is reflected in the survival probability of a quantum state). We think that their interest in both the reactive and nonreactive hydrogen molecules is important for the reason explained above but generalizing their results from only one system to the whole hydrogen-metal systems seems unjustified. They support their generalization even though they accept that e-h pair excitations occur in systems with a deep chemisorption well while their system $\text{H}_2/\text{Pt}(111)$ has a shallow chemisorption well. Again, their result could have helped understand only systems that have a low activation energy to adsorption. There is proof that molecules reacting on metal surfaces excite e-h pairs [18, 20-21]. In these measurements ultrathin metal film Schottky diode detectors are used to measure excited charge carriers as a chemicurrent. The adsorption energy goes into exciting the charge carriers. No chemicurrent was observed when E_{ads} was less than the Schottky barrier, a fact which shows that this energy is efficiently transferred to the electronic degrees of freedom of the substrate.

In our case we indirectly conclude that the translational energy loss depends on incident translational energy but not so much on the vibrational energy. For the cold surface we observe a threshold in the kinetic energy after which the scattered energy decreases significantly. The threshold energy for $\text{H}_2(v=1, J=1)$ is 150 meV and for the

$\text{H}_2(v=0, J=1)$ state is 125 meV. If the surface-adsorbate interaction, in our case $\text{H}_2\text{-Cu}$ (100) system, were very much vibrational-state-dependent then we would observe a significant difference in the scattered energy of the two states. After this threshold energy we notice that the energy loss increases as the incident energy increases. Luntz et al. have pointed out that this could be a non-adiabatic process given that it is velocity dependent. While the whole picture of possible non-adiabatic effects is not well defined we can say that what we observe is a friction effect. We do not observe a higher efficiency for the vibrationally excited state in producing nonadiabatic effects when compared to the ground state. We do not know what to expect exactly because of the lack of calculations related to our specific measurements. Luntz and his coworkers predicted that in an interaction involving a vibrationally excited state the nonadiabatic effects would be higher than one involving a ground vibrational state [25]. We observe elastic scattering and measure the same quantum states incident and scattered, while they calculate inelastic scattering in which the quantum states of incident and scattered molecules are different. Similar reasons may be the origin for many conflicting results in the literature. The system may be different, the surface or the molecule may be different, the quantum states monitored may be different, the process (adsorption or scattering may be different) or the reaction may be different as in the case of this work compared with the work of Luntz and coworkers [25].

Chapter 4

EELS and LEED studies of Cu (100)



O/Cu(100) LEED pattern. $E=333$ eV

There are many ways to probe the surface, some more sensitive than others. X-ray and neutron scattering can be used but their scattering cross-section is very small making them travel into the bulk and the scattered radiation yields a convoluted picture of both bulk and surface. Electrons have higher scattering cross-section, they are scattered 10^3 more times than X-rays [44], and this makes them suitable for surface analysis. Electron spectroscopy has proven to be very useful in situations where other methods show drawbacks. Electrons can be focused to sub-nm scale while light scattering methods can't. The difficulty in providing all the necessary focusing elements for a wide range of wavelengths is another drawback of the optical methods [45].

Here we have used LEED, EELS and Auger electron spectroscopy (AES) to observe the surface structure, to measure surface plasmons and to obtain chemical composition of the surface respectively. We performed these measurements on clean Cu, H/Cu(100) and O/Cu(100).

4.1 CLEAN CU(100)

Copper is a good material to study surface specificity since there are differences in the catalytic activity between the low index single crystal surfaces [46]. Hydrogen adsorption/desorption dynamics and the surface structures as they are covered with oxygen are examples of this [47]. A clean copper surface was prepared as described in section 2.1.

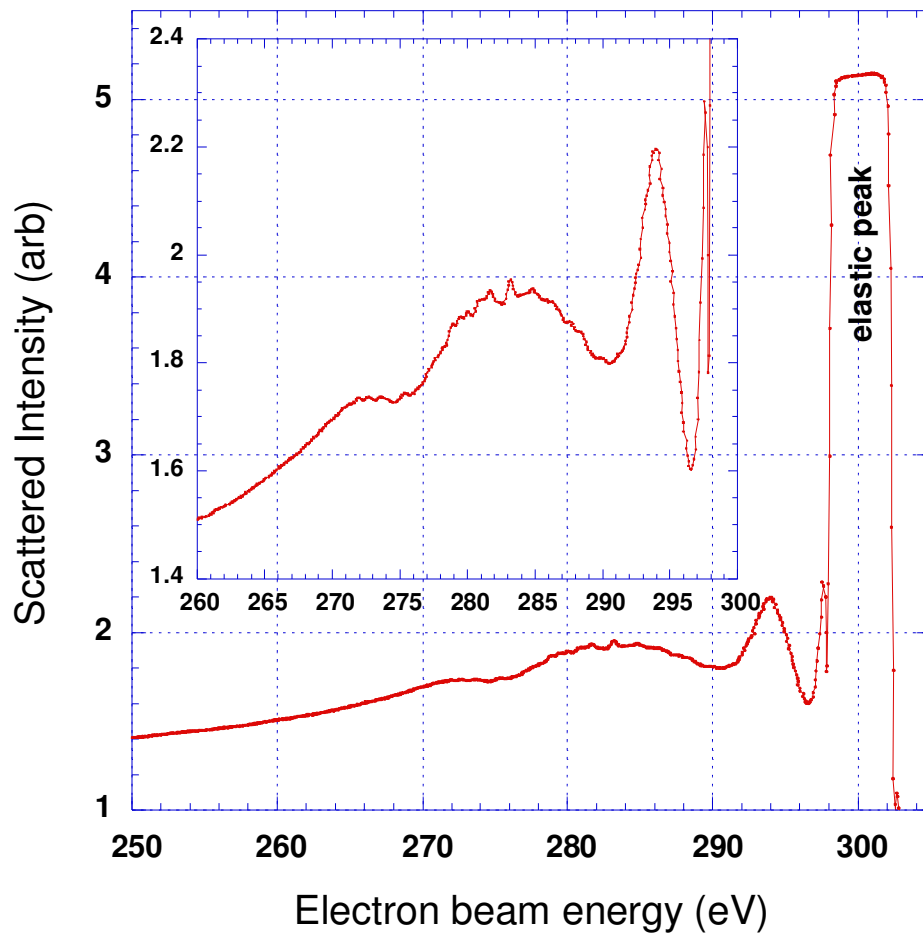


Fig. 4.1 A typical electron energy loss spectrum for copper taken for a primary beam energy of 300 eV at $T=-100^{\circ}\text{C}$. The elastic peak, the surface plasmon at a loss of 6.3 eV and the two bulk plasmons at losses of approximately 18 eV and 28 eV are seen.

We performed LEED, EELS and AES as explained in the experimental section using the reverse view LEED Optics as a retarding field energy analyzer. Sample spectrum is shown in Fig. 4.1. We observed one surface and two bulk plasmon peaks at losses of 6.3 eV, 15.0 eV and 27.5 eV with respect to the elastic peak.

We observed that starting from a clean surface the intensity of the plasmons decreased as the surface was exposed to the electron beam. The surface plasmon decreased in intensity as much as three times as fast as the bulk. The first bulk plasmon intensity decreased significantly too and after some time the feature was hidden in the shoulder of the second bulk peak. The decrease was small but continuous with time and did not seem to be noise or to be related to electron beam instability.

In Fig. 4.2 we can see both the copper Auger electron peak at 58 eV and the electron energy loss peaks decrease in intensity with time. The decrease offers a clear indication that surface plasmon intensity is sensitive, but to what? Clearly, something is changing at the surface. The decrease of the 58 eV Auger peak supports this conclusion. We know that on a clean surface we see a large copper Auger peak and on a contaminated surface the copper peak decreases and the carbon peak, the main indicator for copper contamination, starts growing. We conclude that the surface was getting contaminated.

A similar effect has been reported by Nishizawa et al. [48] and by Shirasawa et al. [49] where they observed defects generated on silicon by scanning tunneling microscopy (STM) and LEED respectively. The first group used STM to observe defects on silicon. From subsequent measurements with Fourier-Transform Infrared (FTIR) spectroscopy and AES they concluded that residual water in their chamber was dissociatively adsorbing on the silicon surface. The second group argued that the high current density of STM can disturb the surface structure and used LEED to monitor the intensity of specific diffraction spots. Both groups attributed the defects of the silicon surface and the decrease of the intensity of the LEED pattern to the dissociative adsorption of the residual water in the vacuum chamber. They had H₂, H₂O, CO and CO₂ in their chamber with

water having the highest partial pressure and given that water has the highest sticking coefficient they concluded that adsorption of water caused the decrease in the LEED intensity. What they did not discuss was whether their observed effects were only in the

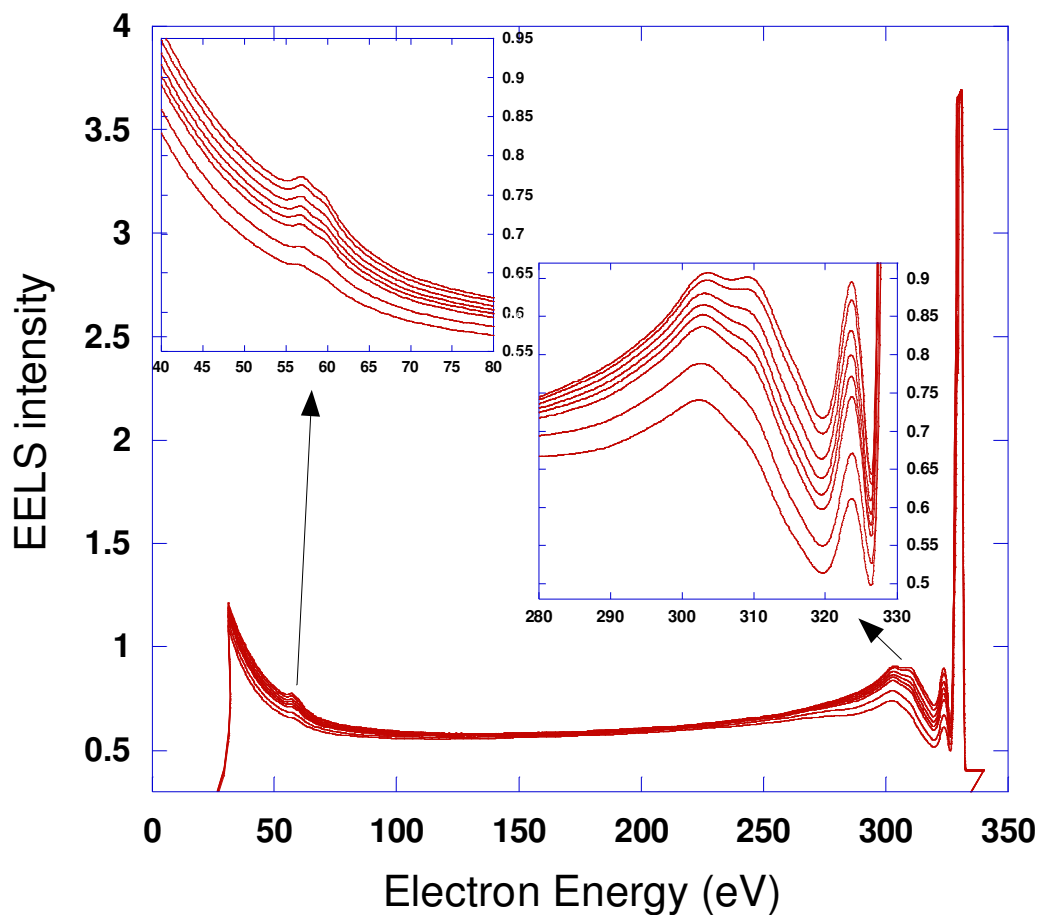


Fig. 4.2 Sample energy loss spectra taken after every hour. The copper Auger electron peak at 58 eV and the EELS peaks are seen. The intensity decreased continuously with time. Each scan took about 8 minutes to acquire.

region probed by STM or the LEED beam. When considering the sticking coefficient of water it is expected that the observed effects would be over the entire surface and if it were residual gas adsorption one would expect water adsorption as a molecule rather than its constituents. Our experimental setup is similar to that of Shirasawa et al. The area exposed to the electron current and the area probed are the same.

At first we thought desorbed contaminants might be coming off of electron gun filament of the LEED optics. To test this we moved the copper sample approximately 0.040" relative to the electron beam and noticed that the intensity of the Auger and EELS peaks increased to the levels of a clean surface. The size of the focus of the electron beam when hitting the sample is estimated to be less than 0.025" in diameter. This convinced us that the observed changes were due to the electron beam itself. We compared EELS spectra of the bulk and the surface plasmon for two different situations: one when the surface was exposed to the electron beam at an energy of 330 eV and one when the surface was not exposed to the electron beam (accomplished by setting the beam energy to 0 eV). The measurements are shown in Fig. 4.3, and were taken every 70 minutes. With the surface exposed to the electron beam the data showed a continuous decrease in the EELS intensity, but the measurements taken every 70 minutes with the surface not exposed did not show any decrease. The surface loss feature is small in these graphs because the surface is not clean. We attributed this decrease of the intensity to electron beam mediated adsorption of residual gasses onto the surface. It will be shown later that the adsorbed residual gas is water by observing the TPD of the EELS peak. Our measurements agree with the result that residual gasses would decrease the intensity following their adsorption on the surface but also suggest that this adsorption is mediated by the electron beam. It may be that the current in both STM and the LEED experiments

induces the adsorption/dissociation of water and this could explain the observations on silicon surfaces. Particularly in the STM experiments the high current density has been a concern because of possible effects it might have on surface structure and recently this current has been proven to be useful in inducing changes in the molecular order of the adsorbates on surfaces [50, 51].

After cleaning the copper surface we measured the EELS in the region of bulk and surface plasmons over a period of approximately 10 hours. The copper surface was kept at $T=-100^{\circ}\text{C}$ the whole time. The data are shown in Fig. 4.4 and Fig 4.5. The offset in the data in Fig 4.4 (the signal for energies above about 334 eV) is not real and has been subtracted from the data in Fig. 4.5. Our first observation is the initial increase of the intensity of the scattered electrons (both the surface and the bulk). This continued for the first 10 minutes. We attributed this to the cleaning of the surface by the electron beam induced desorption of the contaminants. Right after the cleaning the Auger spectra show no contaminants and this makes us believe that the EELS is particularly sensitive to contamination. We were not able to identify these contaminants but one possibility is the residual gasses: CO and CO₂. We excluded water as the desorbing contaminant for reasons that we will explain later more in detail. After the initial increase we observed a continuous decrease in the surface plasmon feature. Overall there is a 70% decrease over a period of 8 hours. As seen in Fig. 4.6 the bulk plasmon features did not change significantly in the first four hours. After about five hours also we see an increase in the rate of intensity loss and this is because the bulk losses are increasing. The bulk features are much wider in energy as they can be seen in the figure thus contributing considerably to the surface feature loss. It is hard to separate the surface from the bulk features but the observed behavior of the features implies that the first 25% of the loss is predominantly

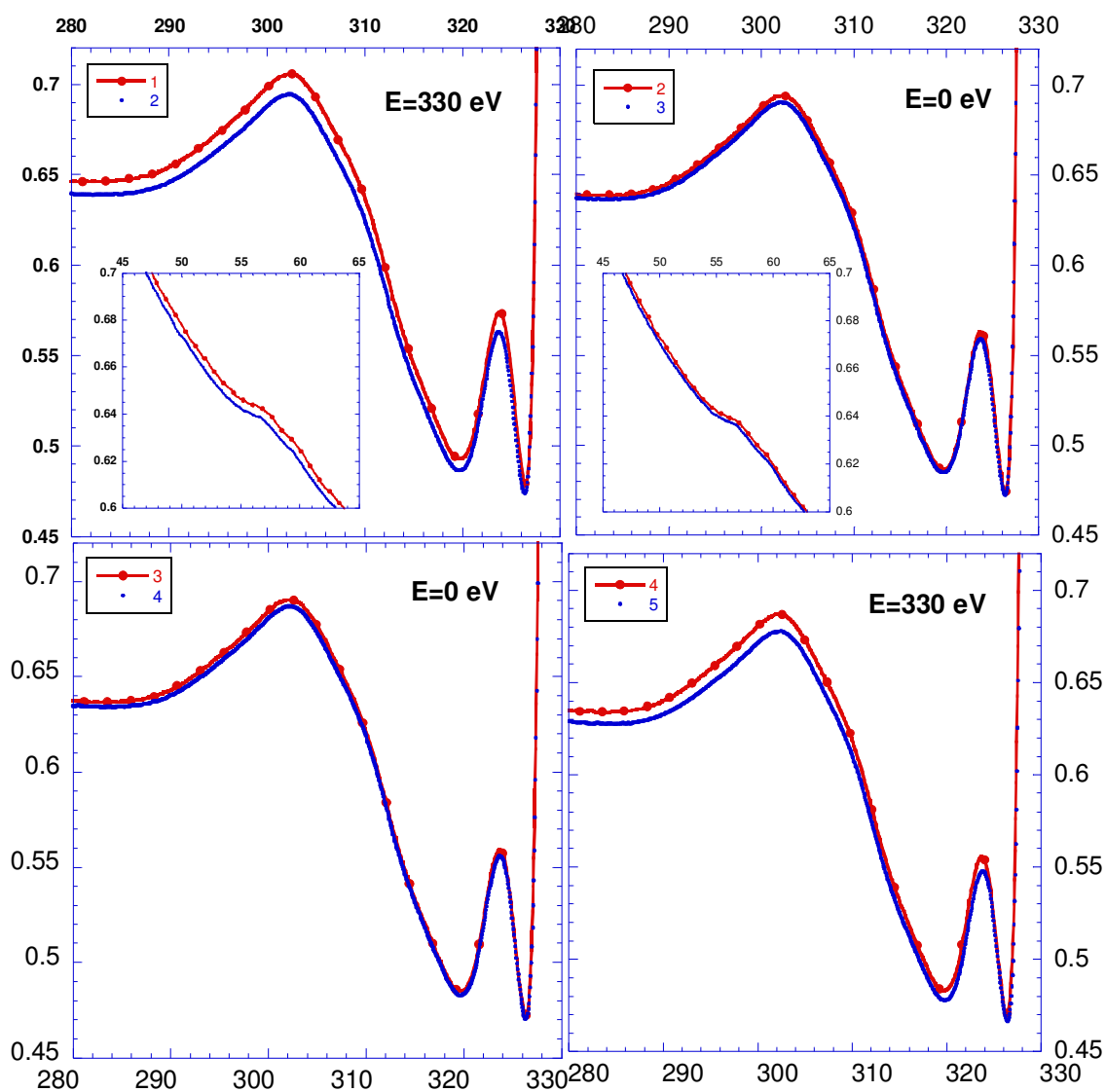


Fig. 4.3 Consecutive energy loss spectra of surface and bulk Plasmon every 70 minutes with $E=330\text{eV}$ and $E=0\text{ eV}$. For the first two the copper Auger peak is shown. 1 vs 2, 2 vs 3, 3 vs 4 and 4 vs 5 are shown with the condition as shown in each graph.

surface loss. One of the well-known and expected drawbacks of electron spectroscopy is the contribution from multiple scattering. Many electrons that would scatter only once from the surface plasmon of a clean surface now are scattered a second time from the contaminants and/or adsorbates and so they will emerge with larger energy losses with respect to the elastic peak. For saturated hydrogen and oxygen covered copper surface the maximum decrease would be approximately 25%. Water is known to adsorb molecularly on copper and desorbs at around -123°C [46]. The 70% decrease can be explained by the adsorption nature of water.

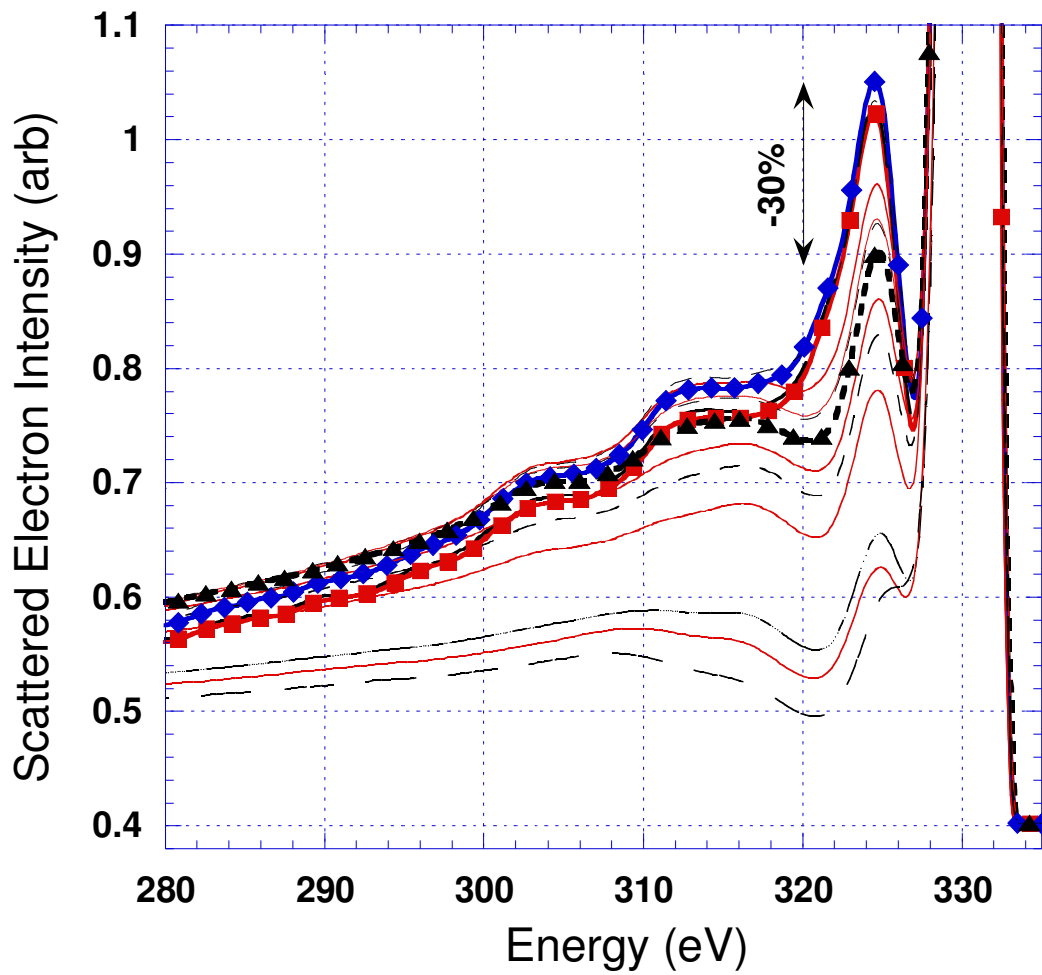


Fig. 4.4 EEL spectrum data taken every one hour. --■-- is the first scan. --◆-- is the scan after 8 minutes. --▲-- is the scan after 4 hours. The decrease of surface plasmon intensity in the first 4 hours is approximately 30%.

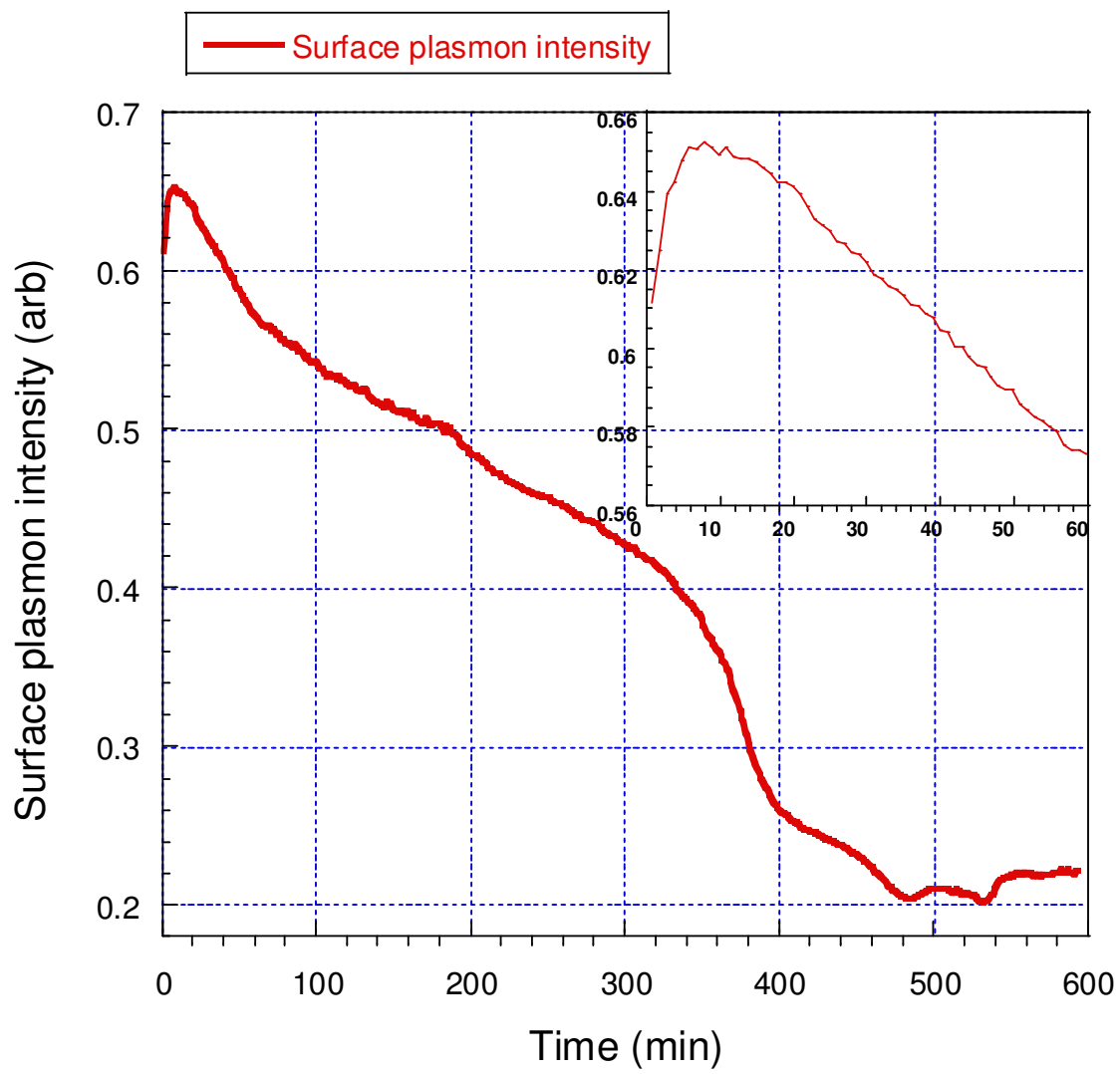


Fig. 4.5 Surface plasmon intensity as a function of time as it is exposed to the electron beam. The background has been subtracted. The inset shows the early time data on an expanded scale.

4.2 H/Cu (100) AND THE VIRTUAL TPD

4.2.1 H/Cu(100) and Copper reconstruction

Chemisorption of hydrogen on metals has been studied extensively because of its many uses. This process is important because it can be applied in many fundamental applications such as catalytic reactions, hydrogen storage, hydrogen-induced embrittlement and fracture in metallurgy [12, 52]. The chemisorption of hydrogen on metal happens by dissociative adsorption and there is no other way except at very low temperature. Hydrogen is known to adsorb molecularly on copper at 10°K such that the rotational states of hydrogen can be monitored. Upon the adsorption of hydrogen on any metal following the creation of metal-H bond a weakening of metal-metal bond is expected [23]. This process is accompanied by layer relaxation or surface reconstruction [52]. Extensive literature has been written about hydrogen adsorption on transition metals but relatively few of them have been focused on copper which has an activation barrier to hydrogen adsorption [53]. Copper reconstruction was among the most recent studied in detail [54]. Hayden et al. proved that hydrogen induced reconstruction of Cu (110) and Chorkendorff et al. did the same for Cu (100). Walters et al. did further careful studies and established a correlation of surface structures with absolute coverage [55].

We studied the H/Cu (100) surface using LEED, EELS, TPD and “virtual TPD”, to be explained below. Dissociative adsorption of hydrogen on copper is an activated process which is reflected in a very small sticking coefficient. The existence of the activation barrier is associated with the completely filled d-band of copper [39]. To practically cover the surface with hydrogen we first dissociate the hydrogen. The hydrogen molecule has a binding energy of 4.5 eV [56] so upon dissociation there are

two hydrogen atoms each with 2.25 eV energy. The clean hydrogen was brought into the chamber through a molybdenum tube with a diameter of 1 cm. The tube had a small hole of about 1 mm through which the hydrogen molecules would be dosed into the chamber. Molecules hit a tungsten foil which is kept at temperatures higher than 2000°C. The sample was approximately 1.5 inch away from the tungsten foil. This configuration gave us an efficient adsorption of hydrogen on copper typically requiring a shorter time or lower chamber exposure when compared to similar efforts reported in the literature.

In our experimental setup, we lack the capability to quantitatively measure LEED intensities and were not able to analyze with precision the loss in the intensity of the LEED pattern of Cu (100) following the absorption from the background. However, we are able to observe qualitative changes in LEED patterns as the surface composition and/or structure is changed. For example, we have observed the LEED pattern for Cu(100) exposed to atomic hydrogen. Hydrogen atoms are not good scatterers [57] (of electrons) and so while we did not, and didn't expect to, see the hydrogen atoms on the LEED pattern we could see the hydrogen induced reconstructions. As hydrogen is adsorbed on copper at a surface temperature of -100°C the surface reconstructs and as the amount of hydrogen exposure increases there is a transition stage where the copper LEED pattern changes from that of a clean surface to one of a reconstructed nature. In this transition stage the copper surface exhibits a streaky pattern which is shown in Fig 4.6.ii. We were able to see a loss in contrast of the early pattern of a reconstructed H/Cu(100). The streaks observed for lower H-atom doses fade away as we observe the LEED pattern over a period of roughly 10 minutes. After streaks are gone, if we translate the sample with respect to the electron beam we see the streaks again and keeping them under electron beam exposure makes them go away again. This again shows once that it

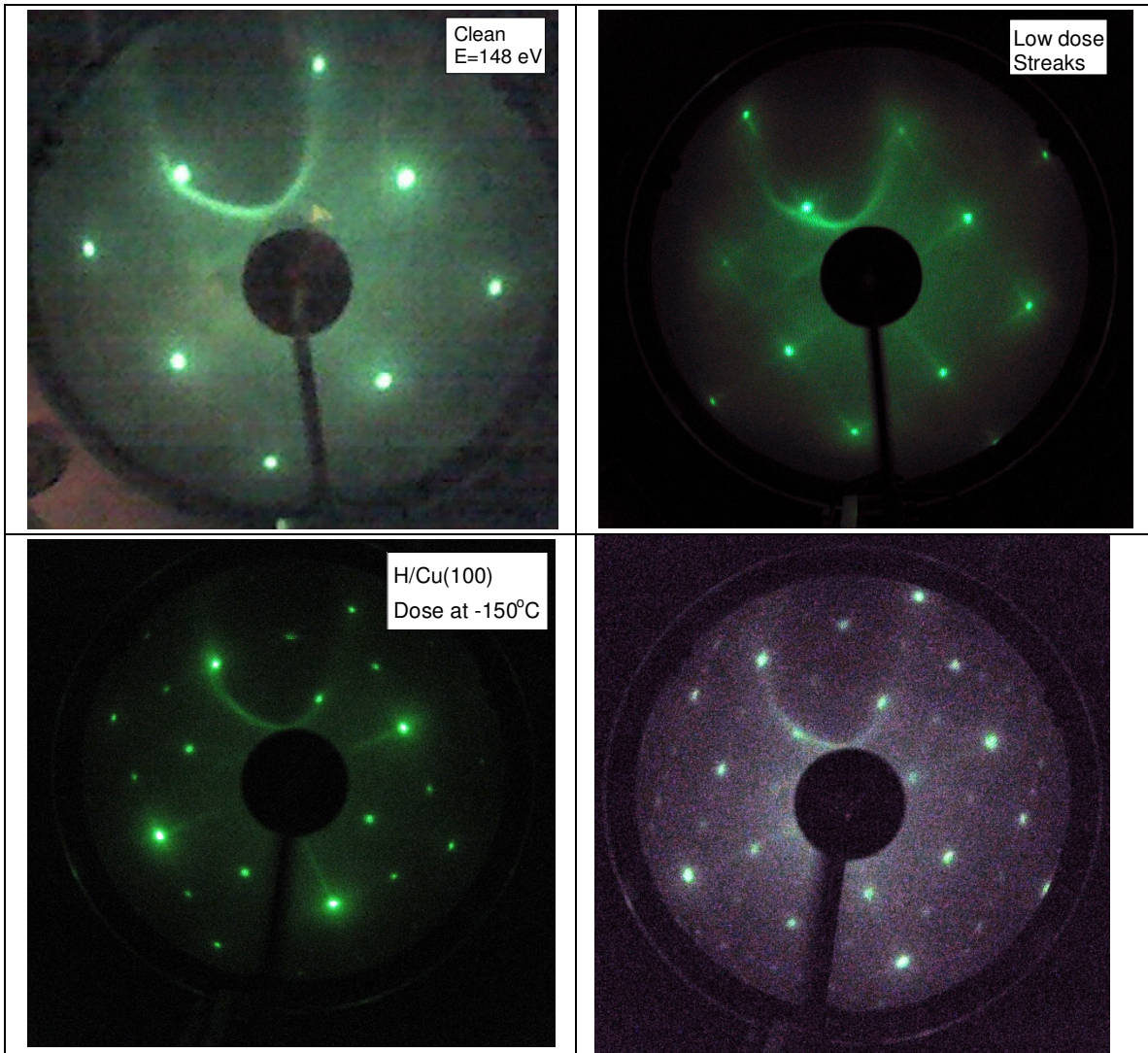


Fig. 4.6 LEED for clean and reconstructed Cu. i) Clean Cu $E=148$ eV. ii) Streaky pattern of Cu(100) LEED just before getting reconstructed. $E_e=120$ eV. iii) Reconstructed Cu (100) upon dosing H atoms at -150°C . $E_e=138$ eV. iv) LEED of H/Cu(100) at $E=89$ eV. Dosed at -100°C .

is the electron beam causing changes on the surface. Other groups have observed reconstructed copper patterns that were unstable under the electron current of the LEED instrument [55]. Our argument is that the streaks are lost because of residual gasses adsorption based on the observed decrease in the surface plasmon peaks as a function of time. The loss of the streaks of hydrogen covered copper might also be because of hydrogen desorption assisted by electrons. This would be in agreement with what electrons have been known to be so good at: desorption of adsorbed molecules and atoms. For this process many models have been proposed. Among these models one explained [58] that an external electron with energy of around 20 eV could ionize an atom adsorbed on the surface. Then a force originating from image charges in the substrate accelerates the atom toward the surface. As it moves in this ionized adsorbate potential curve the atom can pick an electron from the substrate around the point of intersection with the curve for the neutral adsorbate atom and so end up as a neutral atom in a region of very high potential energy and then it will just “roll down” the potential curve and eventually desorbs with an energy in the order of tens of eV.

In Fig 4.6 two different stable copper reconstructions acquired after a higher hydrogen exposure (when compared to streaky pattern exposure) are shown. The first one, p4g reconstruction, is obtained by dosing at -150°C and observed at $E=138$ eV is shown Fig. 4.6.iii. The second one, known in the literature as $(4\sqrt{2} \times 2\sqrt{2})R45^{\circ}$, is obtained by dosing copper surface at -100°C and observed at $E=89$ eV. Walters et al. reported that the dosing temperature was important in deciding the reconstructed LEED patterns and after careful work they stated that -123°C is the limit temperature where the patterns would switch from one to another. They do not give any possible reason for this but we think that this might be related to water adsorption on copper. This reported

transition temperature is the temperature of desorption of water. All three reconstructions would disappear and the LEED would revert to that of clean copper at a temperature of approximately -40°C as we heat the sample. Other groups have observed the same phenomena upon heating a reconstructed copper surface [54].

To find the time needed for one monolayer we use $t = \frac{10^{19}}{F}$ where F is the flux given by the expression: $F_{gas} = \frac{P}{\sqrt{2\pi n_{gas} kT}}$. The times to expose 1 ML of H₂, D₂, O₂ at a base pressure of 10⁻⁶ Torr are calculated and shown on Table 4.1.

Gas	Flux at P=10 ⁻⁶ Torr (molecules m ⁻² s ⁻¹)	Time to 1 ML (sec)
H ₂	1.44x10 ¹⁹	0.7
D ₂	10 ¹⁹	1.0
O ₂	3.6x10 ¹⁸	2.8

Table 4.1 Hydrogen, deuterium and oxygen molecular flux at P=10⁻⁶ Torr and times needed to expose 1ML on Cu(100)

4.2.2 EELS studies and “virtual TPD” of H/Cu(100)

Recently electron spectroscopy is being used in new ways to study matter. For example, Werner successfully used reflection electron energy loss spectroscopy (REELS) to measure the dielectric function of copper [45]. Having established that the EELS

spectra are sensitive to the surface impurities and/or surface adsorbates we extended our measurements to covered copper surfaces prepared in a known manner. We measured the intensity of the surface EELS peak of for clean Cu, H/Cu(100) and O/Cu(100). A decrease of 25% was observed in the intensity of the surface plasmon following hydrogen adsorption. Repeated cycles of cleaning and atomic hydrogen exposure showed that the behavior of the surface plasmon intensity was highly repeatable. Chorkendorff et al. also observed a decrease to a third of the original value of the intensity of the elastic peak in their HREELS experiments for hydrogen covered copper surfaces [59]. As we heated the sample the intensity of the surface peak would increase continuously until it reached the original intensity corresponding to the clean copper. Taking the time derivative of the intensity gave a curve that was very similar to the TPD obtained by mass spectrometry. We call these new curves virtual TPD. The comparison is shown in Fig. 4.7. The curve had a peak temperature which was smaller as the hydrogen exposure to the Cu (100) increased. It is known that the hydrogen desorbs off of copper at lower temperatures as the dosage increases because the hydrogen desorption is a second order process. Comparing the TPD and the virtual TPD convinced us that the integral of the latter ones is linearly dependent of the surface hydrogen coverage. Similar indirect analysis of the surface adsorbates have been reported by different groups using a variety of methods [60-62]. Danişman et al. probed surface coverage using specular helium scattering after correcting the data for the Debye-Waller attenuation. Hu et al. used optical second-harmonic-generation to monitor the hydrogen desorption from Si(001). The advantage of using any of these indirect methods of coverage probing is that unlike mass spectrometry which can measure only one mass now all the desorbing masses can be analyzed at the same time. Also these methods monitor the surface directly and are insensitive to

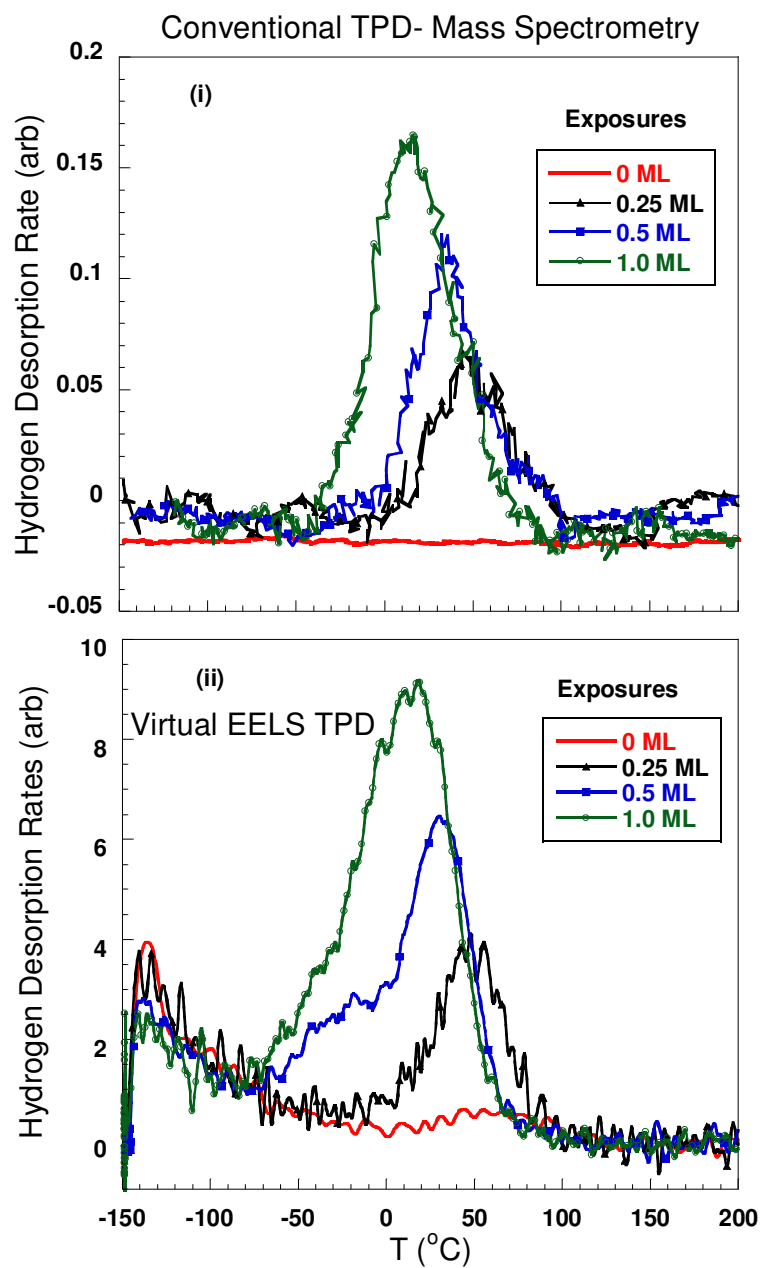


Fig 4.7 (i) Conventional TPD using mass spectrometry. (ii) Virtual TPD obtained by taking the derivative of the intensity of the surface plasmon.

spurious signals that a mass spectrometer might pick up such as desorption from the edges of the sample, sample holder or from heating filaments. The desorption from the edges of the sample can be very misleading for two reasons. First because the area of the copper sample is not negligible when compared to the rim area and secondly they both have the same temperature of desorption. To the best of our knowledge electron scattering has not been used before to probe surface adsorbates in the manner presented here.

Virtual TPD shows the desorption of all of the masses in one spectrum. To identify the masses one can compare the observed peak temperature with known desorption temperatures. When comparing the mass spectrometry TPD and virtual EELS TPD shown in Fig 4.7 we see some differences. The conventional TPD shows no hydrogen signal when dosing amount is zero which makes detecting small desorption difficult. This is what one would expect. The reason is the ubiquity of a high hydrogen background. In the second TPD we see a small signal which is the UHV chamber residual hydrogen adsorbed on the copper surface. The surface adsorbed hydrogen may have been dissociated by the ion gauge filaments. Another difference is the signal observed at peak temperature of about -140°C for the virtual TPD. That observed peak is the residual water desorbing from the surface. Hydrogen for these data was dosed at -150°C surface temperature and it is known experimentally that water adsorbs molecularly on copper surfaces at temperatures below -125°C [46, 63]. This water can adsorb during the time between the dosing and the TPD. It takes approximately 7-8 minutes to rotate the sample from the LEED apparatus to the dosing position and back. Another time factor not to be forgotten is the cooling time after the TPD. It takes 10-20 minutes to cool down the sample from $+450^{\circ}\text{C}$ to -150°C depending on the liquid nitrogen flow rate. In the

previous section we explained how we exposed the clean copper surface to the electron beam and the surface plasmon peak decreased continuously with time. With virtual TPD we have observed that there always is a peak around the desorption temperature of water. To test the effect of the electron beam on the surface we did the following. We cleaned the sample, cooled it down, heated up and cooled it back, exposed to the electron beam for 10 minutes and then performed a virtual TPD. This was done with the sample at a relative vertical position of $z=0.68^\circ$. After that the sample was cooled again and the TPD was repeated now at $z=0.60^\circ$. The plasmon intensity is higher for the non-exposed $z=0.60^\circ$ sample position and the water signal in the TPD was smaller. See Fig 4.8. Comparing the whole temperature range of the two TPD's shows no other possible desorbed molecules and so we attribute the larger amount of water desorption to the electron beam induced dissociation. Andersson et al. also observed electron beam induced dissociative adsorption of water. We were not able to confirm whether it is dissociatively adsorbed or not but we can see that it is water. The second data was then compared to a cleaned sample, heated and cooled twice but this time the cooling time was longer: 20 minutes compared to the previous 10 minutes. The sample cooled at a slower rate shows a larger water desorption feature and an approximately equal hydrogen peak. The third panel of Fig. 4.8 shows repeated measurements with the same cooling rate and at the same sample spot with the only difference being decreased hydrogen desorption.

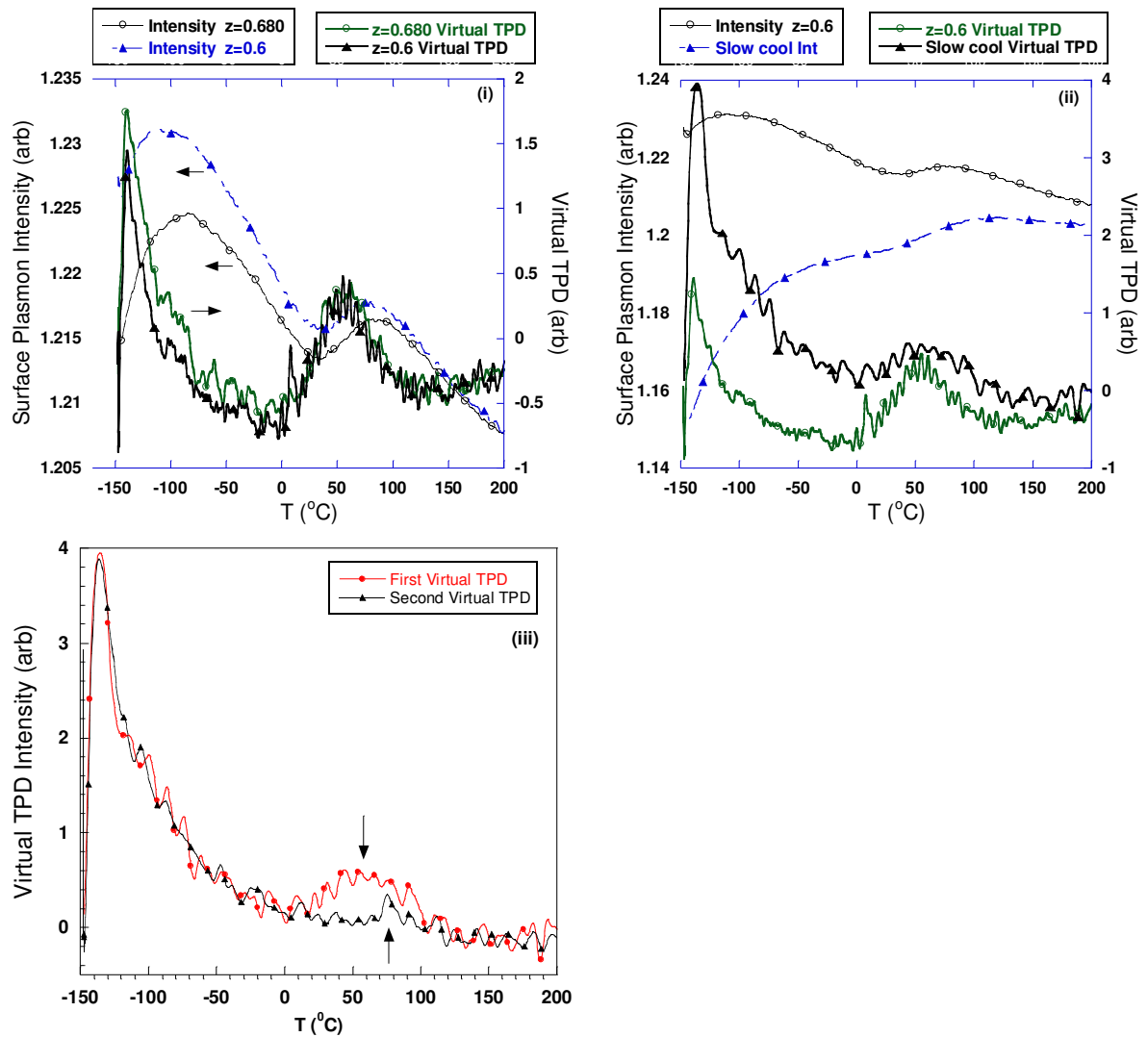


Fig. 4.8 Surface plasmon intensity and Virtual TPD are shown for: (i) Surface cleaned followed by the heating-cooling cycle and exposed to electron beam at $z=0.68''$ for 10 minutes ($-\Theta-$), measurements at $z=0.60''$ with no prior electron beam exposure ($-\blacktriangle-$). (ii) Measurements are compared for different cooling times. Relatively rapid cool down ($-\Theta-$) and slower cool down ($-\blacktriangle-$). (iii) Repeated measurements at the same sample spot. First cycle ($-\bullet-$), second cycle ($-\blacktriangle-$). In each case the cooling time was ≈ 20 min.

Copper has been shown to exhibit unique behavior in hydrogen thermal desorption spectra. Our studies shed more light on this unique behavior. Chorkendorff et al. and Walters et al. showed that for two consecutive desorption spectra from saturated H/Cu(100) the peak in the second spectrum would shift to lower temperatures. We exposed the surface to 50 ML of hydrogen twice, observed well reconstructed copper surfaces both times in LEED and acquired a virtual desorption spectra. We found that the peak in the second one shifted to lower temperature by 10°C. This is called the memory effect where the desorption is dependent on the history of the surface preparation. Then we exposed the surface to 250 ML of hydrogen. This time we observed a LEED pattern characteristic of a clean surface with very strong diffraction spots. This was a surprising observation. Repeated experiments convinced us that exposing the copper surface to a very large hydrogen dose lifts the initial reconstruction. The hydrogen is still present on the surface as was confirmed by both conventional TPD and virtual EELS TPD. A similar effect is reported for Ru(1010) and Re(1010) [52, 64]. Ruthenium and rhenium are very chemically active and both have high sticking probability for molecular hydrogen: $SP \approx 1.0$ and $SP = 0.7$ respectively. After the large reconstruction-lifting exposure, the copper was exposed to 50 ML and this time the TPD shifted by +6°C when compared to the previous 50 ML exposure, that is back towards the result for the first exposure. Another exposure of 50 ML resulted in a TPD shifted by -12°C. All these measurements are shown in Fig. 4.9. So, together with the memory effect for exposures of 50 ML we have a “memory wiping effect” (amnesia effect) of copper as it is exposed to a very large amount of hydrogen followed by flash heating of the surface up to 400°C. Another way to wipe the memory about the preparation history is to clean the sample as we have explained in the experimental section using sputtering with Ar⁺ ions and

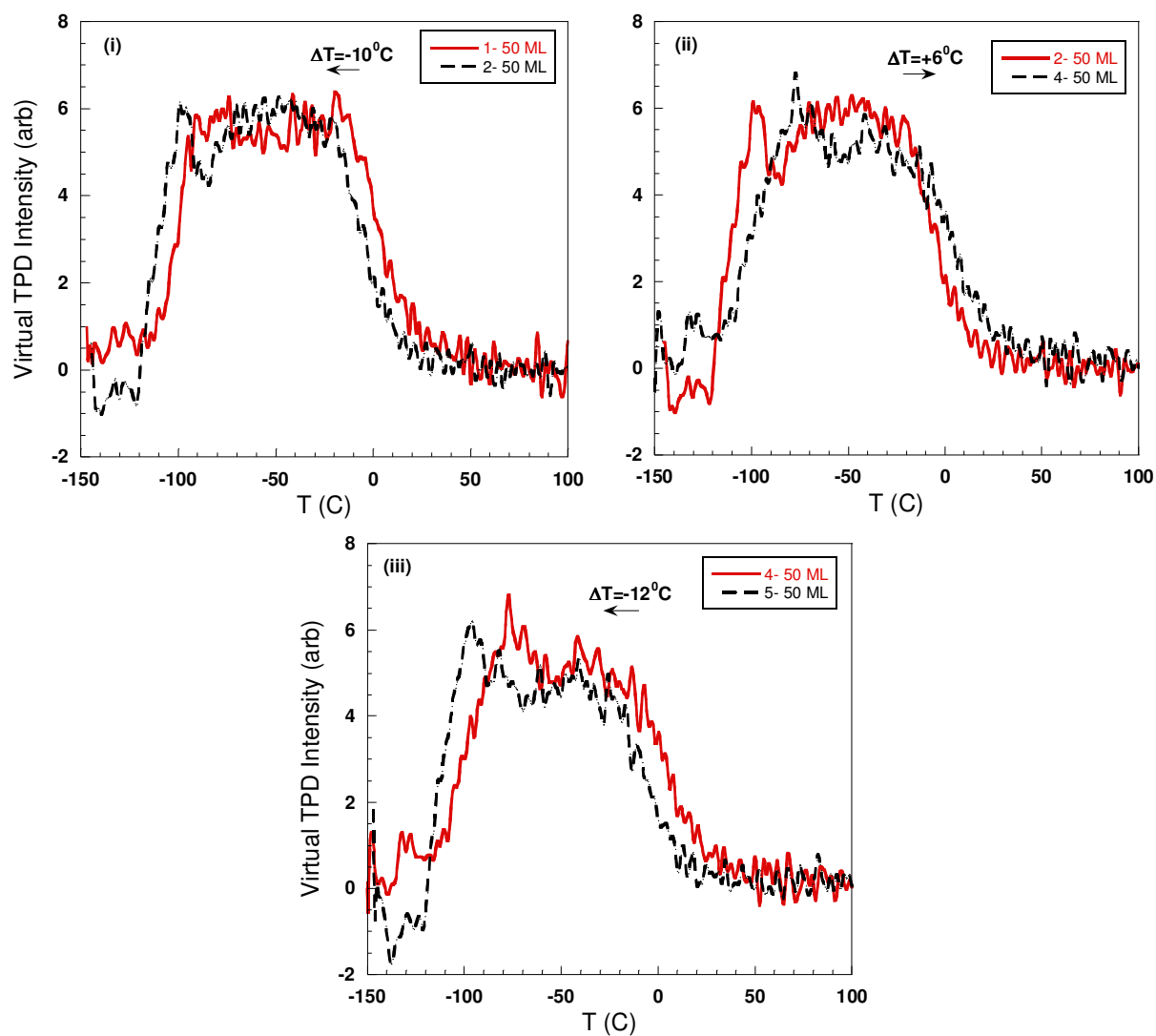


Fig. 4.9 Virtual TPD spectra. (i) Two consecutive TPD after 50 ML H₂ doses. (ii) Two TPD after 50 ML doses with a 250 ML dose in between. (iii) Two consecutive TPD after 50 ML doses.

annealing. The pattern of peak desorption temperatures and their dependence on cleaning/dosing/temperature cycling was highly reproducible.

We claim that we have observed a change in the structure of Cu(100) as a function of hydrogen coverage. A similar direct lifting of the reconstruction has been observed only for metals that have no activation barrier to molecular hydrogen adsorption. Anger et al. could not produce a saturated copper surface mainly because of the energy limit in their molecular beam experiment [39]. (Their maximum beam energy was 0.4 eV.) The reason that Cherkendorff et al. and Walters et al. did not observe the lifting of the reconstruction could be because of the more efficient atomic hydrogen exposure that we have in our experiment. Cherkendorff et al. could observe a reconstructed H/Cu(100) only at exposures above 200 ML. In our experiment we could see a reconstructed surface after 2.5 ML exposure. (In their case they had a copper can where a tungsten filament was mounted out of the sight of the crystal.) Hydrogen exposures are expressed as pressure \times time where the pressure is the H₂ partial pressure, and are not easily converted to H-atom exposure. Hydrogen atoms are very active and may adsorb on any surface they might hit before the copper one. Also the pressure does not count the atoms that stick on the surface. Nienhaus et al. [18, 20] did studies with copper films exposed to atomic hydrogen. They measure the chemi-currents, as they call the charges excited in the metal, as the surface is exposed to hydrogen atoms. They see an almost instantaneous decrease in the measured chemi-current after approximately 30 minutes of atomic hydrogen exposure. We suggest that this decrease might be because of the structural change of the copper crystal, although they propose otherwise.

Another interesting observation in the virtual TPD's was a second wide, sometimes asymmetric peak following doses larger than 250L. This peak is centered at

temperatures 300-370°C. We performed thermal desorption with QMS and observed hydrogen desorbing at 365°C. The virtual TPD ensured us that this hydrogen was desorbing from the sample surface. All the thermal desorption measurements in the literature are done up to a temperature of +120°C. Christmann stated that the surface reconstruction may be regarded as precursor stage for a progressive chemical attack of hydrogen atoms on the bulk, leading to the subsurface site occupation and to the bulk diffusion [52]. We suggest that the large atomic hydrogen exposure and the initial reconstruction have led to a decrease in the difference between the energy levels of adsorbed (surface) hydrogen and those of absorbed (bulk or near surface) hydrogen. Hydrogen is not expected to create any multilayer structure like water. For example, it may be more energy favorable to occupy the subsurface sites and then absorb fully into copper sample. The subsurface and/or absorbed hydrogen may change the activation energy for desorption by lowering it which is observed by many groups as a shift to lower temperatures in the thermal desorption peaks for subsequent equal exposures. So, it may be that this hard-to-notice hydrogen inside the bulk is the cause of the memory effect. Again the memory effect is observed only for saturated surfaces. It is worth remembering that the thermal desorption of hydrogen from Cu(100) is unique, different from Cu(110) and Cu(111), even at low coverages. Anger et al. observed that desorption spectra of large coverages would cross over the spectra of smaller coverages. We find that high exposure to atomic hydrogen followed by thermal desorption up to a high temperature removes the memory effect.

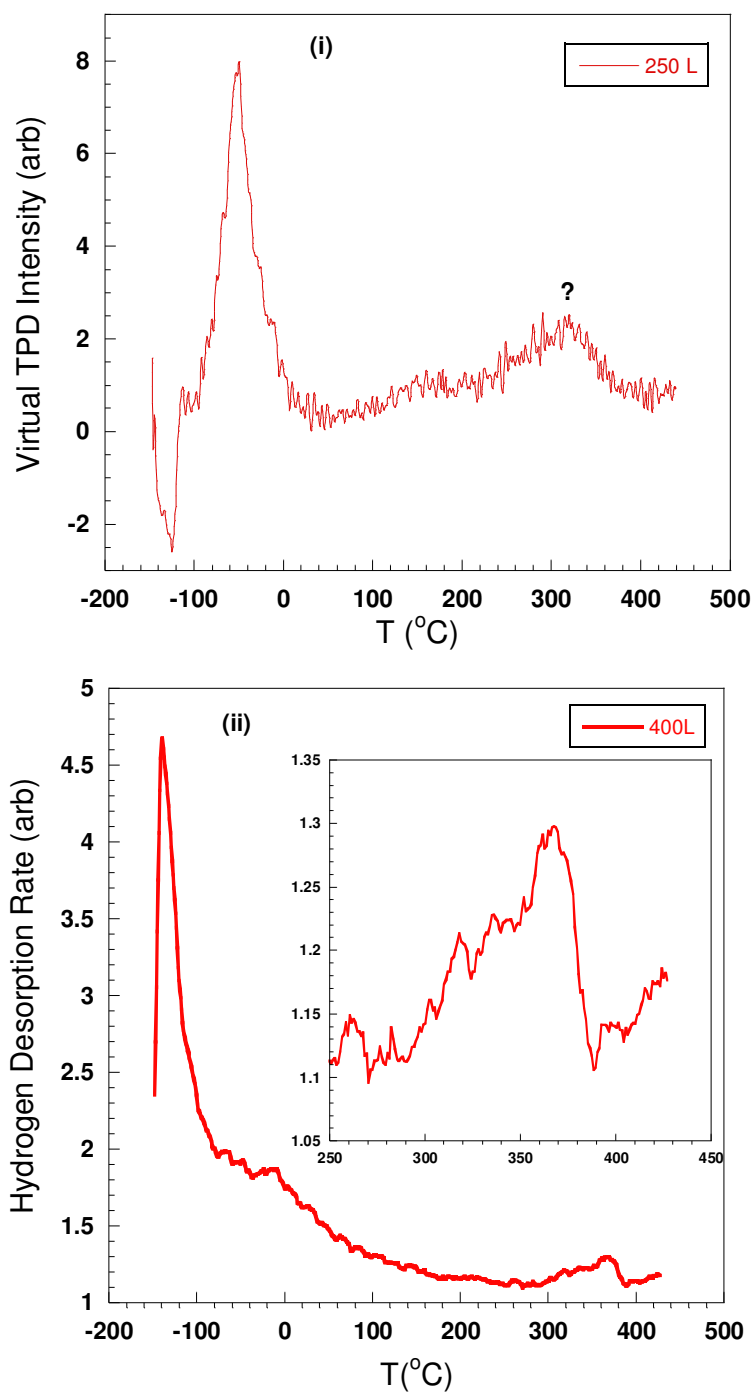


Fig 4.10 (i) Virtual TPD after 250 ML exposure. (ii) Mass spectrometer signal after 400 ML exposure. Desorbed hydrogen can be seen at 365°C .

4.3 O/Cu (100)

The copper-oxygen system has been studied for its importance in heterogeneous catalytic reactions. The full understanding of copper oxidation will help in the fabrication of metal oxides. The early interest was in whether oxygen adsorbs as a molecule or as an atom on copper. At -173°C chemisorbed molecular oxygen has been observed [65], for higher temperatures oxygen adsorbs atomically. Sueyoshi et al. showed that the O/Cu(100) surface can oxidize CO and abstract hydrogen from water [66]. The symmetry of the structures formed upon oxygen adsorption has long been controversial [67]. The structures are a function of coverage and their coexistence has been an unanswered question for more than 20 years. Only recently has the O/Cu(100) system become better understood. Studies using STM, LEED, HREELS, surface x-ray diffraction (SXR), photoelectron diffraction (PhD), transmission electron microscopy (TEM), reflection high energy electron diffraction (RHEED), very-low-energy electron diffraction (VLEED) and analytical electron microscopy have established the structure of oxygen on copper at low and high coverages [67-72].

We exposed Cu (100) to background oxygen at $+100^{\circ}\text{C}$. At this temperature with no added gas exposure no change was observed in the EELS intensity for hours after the cleaning. After dosing oxygen we observed new LEED patterns and oxygen was observed using AES. The observed pattern was the established one observed by other groups: missing row reconstructed $(\sqrt{2} \times 2\sqrt{2})R45^{\circ}$ [68, 72]. The pattern was achieved after exposing 80 ML of oxygen and it did not change as we increased the total exposure up to 1200 ML. The observations are shown in Fig. 4.11. We heated the oxygen covered sample up to 500°C and the reconstructed pattern persisted and the oxygen was still on the surface as confirmed by AES. The LEED pattern got brighter at colder surface

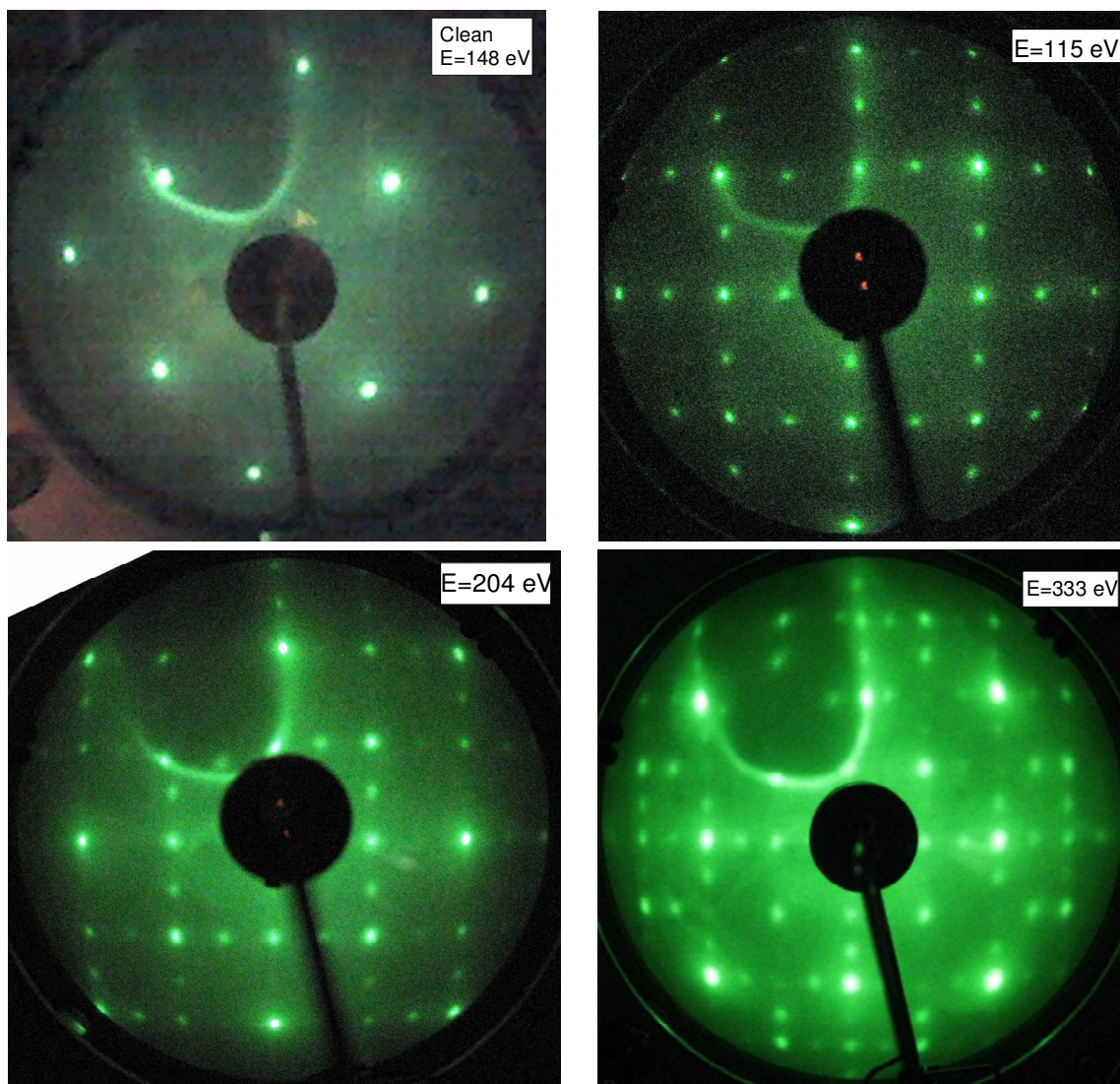


Fig 4.11 LEED of O/Cu(100) at different energies after 460 ML exposure and clean surface pattern.

temperatures. We cooled the oxygen covered copper to -100°C and exposed to atomic hydrogen. After an exposure of 25 ML of H_2 a clean copper LEED pattern was observed and the AES showed no sign of oxygen. Virtual TPD showed desorption of hydrogen similar to the case of very high dose (two desorption peaks similar to the one in Fig. 4.10.i) and no signs of water. After a second 25 ML hydrogen exposure we observed the $(4\sqrt{2} \times \sqrt{2})R45^{\circ}$ H/Cu(100) reconstruction. When comparing these two TPD's we notice that the first one obtained after dosing an oxygen covered surface is characteristic of a surface exposed to a very large amount of hydrogen. Previous studies, explained in the previous section, showed that we get a similar TPD only when the exposure is larger than 250 ML. The second TPD shows a desorption of a saturated surface but obviously less than the first one. So, from this we conclude that more hydrogen is adsorbed on oxygen covered copper than on clean copper. We can say this first based just on the new measurements explained in this section (more hydrogen is desorbed after the first exposure) and second based on the results of this section and the previous one. We know that we cannot observe such typical TPD starting from a clean surface and exposing 25 ML. VTPD are shown in Fig 4.12.i, ii). A similar behavior has been observed by Winkler et al. for hydrogen adsorption on nickel [73]. They observed that pre-adsorption of oxygen on nickel increased the sticking coefficient of hydrogen.

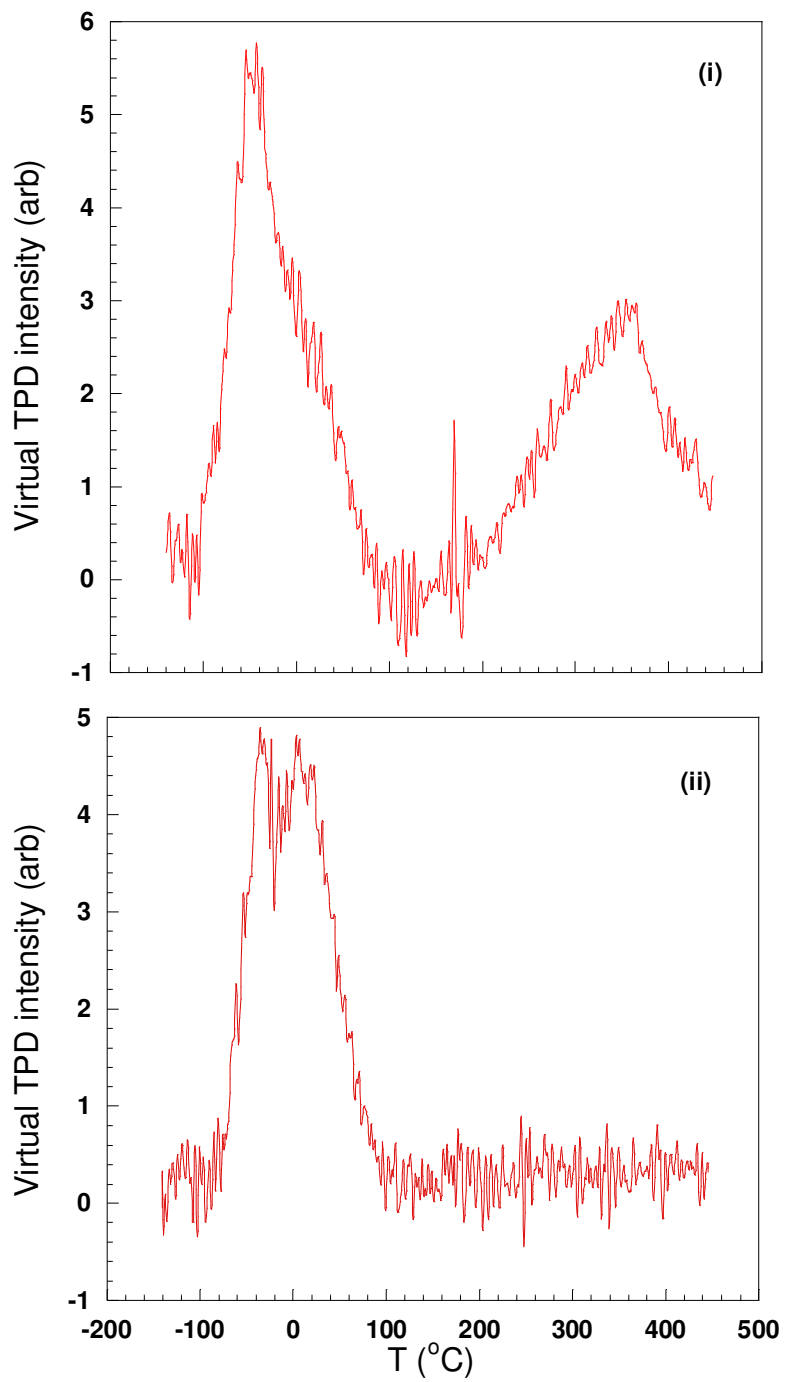


Fig 4.12 (i) Virtual TPD of O/Cu(100) after it is exposed to hydrogen the first time
(ii) Virtual TPD of O/Cu(100) after it is exposed for the second time to hydrogen

Our measurements suggest that oxygen is protecting the surface from the contaminants by blocking adsorption sites. We did not observe water desorption with the surface sensitive TPD. (Here we are talking about the surface sensitive VTPD's which would show a water desorption feature at approximately -125°C . We are not intentionally dosing water on the sample. Only in that case we would be able to observe a desorbing signal higher than the background.) Water adsorbs molecularly on Cu (100) and it might be that the presence of oxygen is not allowing water to adsorb. This could prove very useful in preventing residual gasses contamination in UHV systems. Another interesting result from our experiment is the cleaning of the copper from oxygen by exposing it to atomic hydrogen. The only possible way for this to happen is the oxygen leaving as a water molecule. The standard procedure to clean oxygen from copper is performing the cleaning cycle which includes Ar⁺ ion sputtering and annealing. This whole procedure lasts one hour. Cleaning O/Cu (100) by exposing to atomic hydrogen is faster and can be done at a low temperature. Removing the hydrogen afterwards requires a flash heating. This cleaning procedure can save time and can make easier the manufacturing steps of metal oxides. Similar cleaning method is used by researchers to remove oxygen from silicon. Researchers are interested in cleaning silicon at lower temperatures and for this they expose it to atomic hydrogen at temperatures lower than 800°C [74].

Chapter 5

Conclusions

In the first part of this thesis, quantum state resolved energy losses due to scattering from Cu (100) were measured. In the second part clean Cu (100), H/Cu (100) and O/Cu (100) surfaces were studied using electron spectroscopy methods.

Translational energy loss was measured for elastically scattered H_2 ($v=0, J=1$) and H_2 ($v=1, J=1$) quantum states as a function of incident translational energy at two different surface temperatures, 173 K and 573 K. For the cold surface temperature measurements, energy losses can be explained using the Baule equation for incident energies below 150 meV for the vibrationally excited state and below 125 meV for the ground vibrational state. Data fitted to the Baule equation showed that H_2 ($v=0, J=1$) quantum state exchanges energy with an effective surface mass of 0.5 times the mass of one copper atom ($0.5M_{Cu}$) and H_2 ($v=1, J=1$) quantum state exchanges energy with an effective mass of $0.7M_{Cu}$ from the surface. The data showed that the translational energy loss depends more on incident translational energy and to a lesser extent on the vibrational state. After a threshold energy where the Baule equation no longer holds, the fractional energy loss increases with the incident energy. Such behavior indicates that the scattering process may be nonadiabatic. An electronic friction model developed by Luntz and coworkers might explain this energy loss.

For the high surface temperature, the energy loss for the two measured quantum states can be explained by the Baule equation only for energies smaller than about 120 meV. Data fitted showed that the ($v=1, J=1$) quantum state exchanges energy with an

effective mass of $0.5 \times M_{\text{Cu}}$ and the ($v=0, J=1$) quantum state exchanges energy with an effective mass of $0.7 \times M_{\text{Cu}}$ from the surface.

EELS experiments showed that surface plasmon intensity is very sensitive to surface contaminants and/or adsorbates. Decrease in the surface plasmon intensity is linked to the residual water adsorption following electron beam induced dissociation. The first 25-30% of the decrease of the SP intensity is characteristic to the surface only. Saturation of Cu (100) surface with hydrogen or oxygen decrease the SP intensity by 25%.

Surface reconstruction following the hydrogen atom exposure was observed using LEED. Some of these reconstructions were not stable under the LEED electron gun exposure. The increase in the SP intensity showed that reconstruction is lifted because of electron beam induced desorption of the adsorbed hydrogen.

Surface sensitive only virtual temperature programmed desorption (VTPD) was developed and applied in the experiment.

For H/Cu (100) a unique memory effect has been observed. Prolonged exposure to atomic hydrogen showed a lifting of the reconstruction of H/Cu(100). It was shown that the memory effect can be removed in two ways. One is cleaning of the sample using Ar⁺ ion sputtering and annealing to 600°C. The other is by dosing the surface with atomic hydrogen with high exposures and then heating up to 450°C.

Oxygen covered copper proved to be free of contaminants and this is explained by the unavailability of adsorption sites. Cleaning of oxygen by atomic hydrogen at temperatures lower than -100°C was shown. It is found that the presence of oxygen on the surface increased the amount of hydrogen adsorbed on Cu (100).

References

- [1] Greg O. Sitz. Gas Surface Interactions Studied with State-Prepared Molecules. Reports on Progress in Physics **65** 1165, 2002.
- [2] Drew A. McCormack, Geert-Jan Kroes, Roar A. Olsen, Jeroen A. Groeneveld, Joost N. P. van Stralen, Evert Jan Baerends and Richard C. Mowrey. Quantum dynamics of the dissociation of H₂ on Cu(100): Dependence of the site-reactivity on initial rovibrational state. The Royal Society of Chemistry. Faraday Discuss. **117** 109, 2000; M. F. Somers, D. A. McCormack, G. J. Kroes, R. A. Olsen, E. J. Baerends and R. C. Mowrey. Signatures of Site-Specific Reaction of H₂ on Cu (100). Journal of Chemical Physics **117** 6673, 2002.
- [3] John C. Tully Theories of the Dynamics of Inelastic and Reactive Processes at Surfaces. Annu. Rev. Phys. Chem. **31** 319, 1980.
- [4] Leah C. Shackman and GOS "Scattering of D₂ from Cu(100) and Pd(111)", J. Chem. Phys. **123**, 064712 (2005)
- [5] Axel Gross, Steffen Wilke and Matthias Scheffler. Six-dimensional quantum dynamics of adsorption and desorption of H₂ at Pd(100)" no need for a molecular precursor adsorption state. Surface Science, **357** 614, 1996.
- [6] Leah C. Shackman and GOS "Rotationally Inelastic Scattering of HD from Cu(100) and Pd(111)", J. Chem. Phys. **122** (2005) pp 114702-1-5.
- [7] Axel Gross, Steffen Wilke and Matthias Scheffler. Six-Dimensional Quantum Dynamics of Adsorption and Desorption of H₂ at Pd(100): Steering and Steric Effects. Phys. Rev. Lett. **75** 2718, 1995; M. Beutl, J. Lesnik, K. D. Rendulic, R. Hirschl, A.

Eichler, G. Kresse and J. Hafner. There is a True Precursor for Hydrogen after all: The System $\text{H}_2/\text{Pd}(100)$ +Subsurface V. Chem. Phys. Lett. **342** 473, 2001.

[8] J. C. Tully Chemical dynamics at metal surfaces. Annu. Rev. Phys. Chem. **51** 153, 2000.

[9] M. Alcudin, R. Diez Muino, H. F. Busnengo and A. Salin. Why N_2 molecules with thermal energy abundantly dissociate on $\text{W}(100)$ and not on $\text{W}(110)$. Phys. Rev. Lett **97** 056102, 2006.

[10] T. Mitsui, M. K. Rose, E. Fomin, D. F. Ogletree, and M. Salmeron. Dissociative hydrogen adsorption on palladium requires aggregates of three or more vacancies. Nature **422** 705, 2003.

[11] Stephen Holloway. The Active Site for Dissociative Adsorption of H_2 : Was Langmuir Right? Surface Science **540** 1, 2003.

[12] G. J. Kroes. Six-dimensional Quantum Dynamics of Dissociative Chemisorption of H_2 on Metal Surfaces. Progress in Surface Science 1-85 1999.

[13] W. Dong and J. Hafner. H_2 Dissociative Adsorption on $\text{Pd}(111)$. Physics Review B **56** 15396, 1997.

[14] Cynthia M. Friend. Catalysis on Surfaces. Scientific American 74 1993.

[15] Michael Gostein and GOS, Rotational state-resolved sticking coefficients for H_2 on $\text{Pd}(111)$: Testing dynamical steering in dissociative adsorption, J. Chem. Phys. **106** 7378, 1997; Michael Beutl, Manfred Riedler and Klaus D. Rendulic. Strong rotational effects in the adsorption dynamics of $\text{H}_2/\text{Pd}(111)$: Evidence for Dynamical Steering Chemical Physics Letters **247** 249 1995.

[16] M. Persson and B. Hellsing. Electronic Damping of Adsorbate Vibrations on Metal Surfaces. Physical Review Letters **49** (9) 662, 1982.

- [17] David C. Langreth. Energy Transfer at Surfaces: Asymmetric Line shapes and the Electron-Hole-Pair Mechanism. *Phys. Rev. Lett.* **54** 126, 1985.
- [18] H. Nienhaus, H.S. Bergh, B. Gergen, A. Majumdar, W. H. Weinberg and E. W. McFarland. Electron-hole pair creation at Ag and Cu surfaces by adsorption of atomic hydrogen and deuterium. *Phys. Rev. Lett.* **82** 446, 1999.
- [19] N. H. Nahler, J. D. White, J. LaRue, D. J. Auerbach and A. M. Wodtke. Inverse velocity dependence of vibrationally promoted electron emission from a metal surface. *Science* **321** 1191, 2008.
- [20] Hermann Nienhaus, H. S. Berg, Brian Gergen, W. Henry Weinberg and Eric W. McFarland. Ultrathin Cu Films on Si(111): Schottky barrier formation and sensor applications. *J. Vac. Sci. Technol. A* **17** 1683, 1999.
- [21] Brian Gergen, Hermann Nienhaus, W. Henry Weinberg and Eric W. McFarland. Chemically Induced Electronic Excitations at Metal Surfaces. *Science* **294** 2521, 2001.
- [22] B. Hammer and J. K. Nørskov. Why Gold is the Noblest of all the Metals. *Nature* **376** 238, 1995.
- [23] J. Harris and S. Andersson. H₂ Dissociation at Metal surface. *Phys. Rev. Lett.* **55** 1583, 1985.
- [24] A. C. Luntz and M. Persson. How adiabatic is activated adsorption/associative desorption? *J. Chem. Phys.* **123** 074704, 2005.
- [25] A. C. Luntz, M. Persson and GOS "Theoretical evidence for nonadiabatic vibrational deexcitation in H₂ (D₂) scattering from Cu(100)", *J. Chem. Phys.* **124**, 091101, 2006.
- [26] J. P. Toennies. Serendipitous Meanderings and Adventures with Molecular Beams. *Annu. Rev. Phys. Chem.* **55** 1, 2004.

- [27] Dudley R. Herschbach. Molecular Dynamics of Elementary chemical Reactions. Nobel Lecture. 8 December 1986.
- [28] E. E. Marinero, C. T. Rettner and R. N. Zare. Quantum-State-Specific Detection of Molecular Hydrogen by Three-Photon Ionization. *Phys. Rev. Lett.* **48** 1323, 1982.
- [29] Instruction Manual: Reverse View LEED Optics Models RVL 6-120 and 8-120. Princeton Research Instruments.
- [30] Elizabeth Watts, GOS, D. A. McCormack, G. J. Kroes, R. A. Olsen, J. A. Groeneveld, J. N. P. van Stralen, E. J. Baerends, and R. C. Mowrey, Rovibrationally inelastic scattering of ($v=1, J=1$) H_2 from Cu(100): Experiment and Theory, *J. Chem. Phys.* **114** 495, 2001.
- [31] Elizabeth Watts and GOS, State-to-state scattering in a reactive system: $H_2(v=1, J=1)$ from Cu(100), *J. Chem. Phys.* **114** 4171, 2001.
- [32] P. Rivière, A. Salin, F. Martin. The role of molecular rotation in activated dissociative adsorption on metal surfaces. *J. Chem. Phys.* **124** 084706, 2006.
- [33] G. P. Brivio and R. B. Grimley. Non-Adiabatic Processes in Adsorption/Desorption Phenomena. *Surface Science* **89** 226, 1979.
- [34] H. A. Michelsen, C. T. Rettner, D. J. Auerbach and R. N. Zare. Effect of rotation on the translational and vibrational energy dependence of the dissociative adsorption of D_2 on Cu (111). *J. Chem. Phys.* **98** 8294, 1993; H. A. Michelsen and D. J. Auerbach. A Critical Examination of Data on the Dissociative Adsorption and Associative Desorption of Hydrogen on Copper Surfaces. *J. Chem. Phys.* **94** 7502, 1991.
- [35] C. T. Rettner, H. A. Michelsen and D. J. Auerbach. Quantum-state-specific dynamics of the dissociative adsorption and associative desorption of H_2 at a Cu (111) surface. *J. Chem. Phys.* **102** 4625, 1995.

- [36] R. R. Smith, D. R. Killelea, D. F. DelSesto and A. L. Utz. Preference for Vibrational over Translational Energy in a Gas-Surface Reaction. *Science* **304** 992, 2004.
- [37] Jonghyuk Kim. Quantum State-Resolved Studies of Sticking and Elastic Scattering of H₂ from Cu(100). PhD thesis. The University of Texas at Austin 2006.
- [38] Andrew Zangwill. *Physics at Surfaces*. Cambridge University Press, New York 1988.
- [39] G. Katz, Y. Zeiri, R. Kosloff, Role of Vibrationally Excited NO in Promoting Electron Emission When Colliding with a Metal Surface: A Nonadiabatic Dynamic Model *J. Phys. Chem. B* **109** 18876, 2005.
- [40] G. Anger, A. Winkler and K. D. Rendulic. Adsorption and desorption kinetics in the systems H₂/Cu(111), H₂/Cu(110) and H₂/Cu(100). *Surface Science* **220** 1, 1989.
- [41] Pablo Nieto, Ernst Pijper, Daniel Barredo, Guillaume Laurent, Roar A. Olsen, Evert-Jan Baerends, Geert-Jan Kroes and Daniel Farias. Reactive and Nonreactive Scattering of H₂ from a metal surface is electronically Adiabatic. *Science* **312** 86, 2006.
- [42] J. I. Juaristi, M. Alducin, R. Díez Muiño, H. F. Busnengo, and A. Salin. Role of electron-hole pair excitation in the Dissociative Adsorption of Diatomic Molecules on Metal Surfaces. *Phys. Rev. Lett.* **100** 116102, 2008.
- [43] A. C Luntz, I Makkonen, M. Persson, S. Holloway, D. M. Bird and M. S. Mizielinski. Comment on “Role of electron-hole pair excitation in the Dissociative Adsorption of Diatomic Molecules on Metal Surfaces.” *Phys. Rev. Lett.* **102** 109601, 2009; J. I. Juaristi, M. Alducin, R. Díez Muiño, H. F. Busnengo, and A. Salin. Reply *Phys. Rev. Lett.* **102** 109602, 2009.
- [44] Martin Prutton. *Introduction to Surface Science*. Oxford University Press, New York 1994.

- [45] Wolfgang S. M. Werner. Optical Constants of Cu Measured with Reflection Electron Energy Loss Spectroscopy (REELS). *Surface Science* **600** L250, 2006.
- [46] A. Spitzer, A. Ritz and H. Lüth. The adsorption of H₂O on Cu(100) surfaces. *Surface Science* **152** 543, 1985.
- [47] A. Spitzer and H. Lüth. The Adsorption of Oxygen on Copper Surfaces II. Cu(111). *Surface Science* **118** 136, 1982.
- [48] Masayasu Nishizawa, Tetsuji Yasuda, Satoshi Yamasaki, Kazushi Miki, Masanori Shinohara, Nozomu Kamakura, Yasuo Kimura and Michio Niwano. Origin of type-C defects on the Si(100)-(2×1) surface. *Physical Review B* **65** 161302(R) 2002.
- [49] Tetsuroh Shirasawa, Seigi Mizuno, Hiroshi Tochihara. Electron-Beam-Induced Disorder of the Si(001)-c(4×2) Surface Structure. *Physics Review Letters* **94** 195502 2005.
- [50] J. I. Pascual, N. Lorente, Z. Song, H. Conrad and H.-P. Rust. Selectivity in vibrationally mediated single-molecule chemistry. *Nature* **423** 525, 2003.
- [51] N Lorente, R Rurali and H Tang. Single-molecule manipulation and chemistry with the STM. *J. Phys.: Condens. Matter* **17** S1049, 2005.
- [52] Klaus Christmann. Some General Aspects of Hydrogen Chemisorption on Metal Surfaces. *Progress in Surface Science* **48** 15, 1995.
- [53] B. E. Hayden, D. Lackey and J. Schott. A Vibrational Study of the Hydrogen Induced Reconstructions on Cu (110). *Surface Science* **239** 119, 1990.
- [54] I. Chorkendorff and P. B. Rasmussen. The p4g or pgg Reconstruction on Cu(100). *J. Phys.: Condens. Matter* **3** S107, 1991.

- [55] C. F. Walters, D. B. Poker, D. M. Zehner and E. W. Plummer. The Deuterium-Induced Reconstruction of Cu(100): Correlations of Surface Structures with Absolute Coverage. *Surface Science* **312** L759, 1994.
- [56] David R. Lide. *CRC Handbook of Chemistry and Physics*. CRC Press 1995.
- [57] Klaus Müller. Hydrogen-Induced Reconstruction of Transition Metal Surfaces. *Progress in Surface Science*. **42** 245, 1993.
- [58] P. R. Antoniewicz. Model for Electron- and Photon-Stimulated Desorption. *Phys. Rev. B* **21** 3811, 1980.
- [59] I. Chorkendorff and P. B. Rasmussen. Reconstructions of Cu (100) by Adsorption of Atomic Hydrogen. *Surface Science* **248** 35, 1991.
- [60] Mehmet F. Danişman, Loredana Casalis, Gianangelo Bracco and Giacinto Scoles. Structural Investigation of Monolayers Prepared by Deposition of (CH₃S)₂ on the (111) Face of Single-Crystal Gold. *J. Phys. Chem. B* **106** 11771, 2002.
- [61] David J. Lavrich, Sean M. Wetterer, Steven L. Bernasek and Giacinto Scoles. Physisorption and Chemisorption of Alkanethiols and Alkyl Sulfides on Au(111). *J. Phys. Chem. B* **102** 3456, 1998.
- [62] X. F. Hu, Z. Xu, D. Lim, M. C. Downer, P. S. Parkinson, B. Gong, G. Hess and J. G. Ekerdt. In Situ Optical Second-Harmonic-Generation Monitoring of Disilane Adsorption and Hydrogen Desorption During Epitaxial Growth on Si(001). *Appl. Phys. Lett.* **71** 1376, 1997.
- [63] K. Andersson, A. Gómez, C. Glover, D. Nordlund, H. Öström, T. Schiros, O. Takahashi, H. Ogasawara, L. G. M. Pettersson and A. Nilsson. Molecularly Intact and

Dissociative Adsorption of Water on Clean Cu (110): A Comparison with the Water/Ru(001) System. *Surf. Sci.* **585** L183, 2005.

[64] G. Lauth, E. Schwarz and K. Christmann. The Adsorption of Hydrogen on a Ruthenium (1010) Surface. *J. Chem. Phys.* **91** 3729, 1989.

[65] A. Spitzer and H. Lüth. The Adsorption of Oxygen on Copper Surfaces I. Cu(100) and Cu (110). *Surface Science* **118** 121, 1982.

[66] Tsuyoshi Sueyoshi, Takehiko Sasaki and Yasuhiro Iwasawa. Oxygen Atoms on Cu(100) Formed at 100K, Active for CO Oxidation and Water-Hydrogen Abstraction, Characterized by HREELS and TPD. *J. Phys. Chem. B* **101** 4648, 1997.

[67] Ch. Wöll, R. J. Wilson, S. Chiang, H. C. Zeng and K. A. R. Mitchell. Oxygen on Cu(100) Surface Structure Studied by Scanning Tunneling Microscopy and by Low-Energy-Electron-Diffraction Multiple-Scattering Calculations. *Physical Review B* **42** 11926, 1990.

[68] M. Kittel, M. Polcik, R. Terborg, J. -T. Hoefl, P. Baumgärtel, A. M. Bradshaw, R. L. Toomes, J. -H. Kang, D. P. Woodruff, M. Pascal, C. L. A. Lamont and E. Rotenberg. The Structure of Oxygen on Cu(100) at Low and High Coverages. *Surface Science* **470** 311, 2001.

[69] K. Lahtonen, M. Hirsimäki, M. Lampimäki and M. Valden. Oxygen Adsorption-Induced Nanostructures and Island Formation on Cu(100): Bridging the Gap Between the Formation of Surface Confined Oxygen Chemisorption layer and Oxide Formation. *The Journal of Chemical Physics* **129**, 124703 2008.

- [70] Takaya Fujita, Yuji Okawa, Yuji Matsumoto and Kenichi Tanaka. Phase Boundaries of Nanometer Scale $c(2 \times 2)$ -O Domains on the Cu(100) Surface. *Physical Review B* **54** 2167, 1996.
- [71] I. Merrick, J. E. Inglesfield and H. Ishida. Electronic Structure and Surface Reconstruction of Adsorbed Oxygen on Copper (001). *Surface Science* **551** 158, 2004.
- [72] M. J. Harrison, D. P. Woodruff and J. Robinson. Adsorbate-Induced Surface Reconstruction and Surface-Stress Changes in Cu(100)/O: Experiment and Theory. *Physical Review B* **74** 165402, 2006.
- [73] A. Winkler and K.D. Rendulic. Adsorption Kinetics for Hydrogen Adsorption on Nickel and Coadsorption of Hydrogen and Oxygen. *Surface Science* **118** 19, 1982.
- [74] A. Abmuth, T. Stimpel-Lindner, O. Senfleben, A. Bayerstadler, T. Sulima, H. Baumgärtner and I. Eisele, The Role of Atomic Hydrogen in Pre-Epitaxial Silicon Substrate Cleaning. *Applied Surface Science* **253** 8389, 2007.

Vita

Arban Uka was born in Kruja, Albania on August 27, 1980, the son of Haki Uka and Lirie Uka. After graduating from Mehmet Akif High School he attended Middle East Technical University in Ankara, Turkey. The summer of his junior year and the senior year he did research in the field of optical spectroscopy of semiconductors at Bilkent University. He received degrees Bachelor of Science in Physics and Math in August 2002. In the fall of 2002 he entered The Graduate School at The University of Texas at Austin. In August 2007 he married Ana Bulku.

Permanent address: Rruga Aleksander Goga, Lagja 18,

Pallati 989 Durres Albania

This dissertation was typed by the author.